RNAi-based screen for pigmentation in *Drosophila melanogaster* reveals regulators of brain dopamine and sleep

Samantha L Deal[1,2,3], Danqing Bei[2,4], Shelley B Gibson[2,4], Harim Delgado-Seo[2,5], Yoko Fujita[2,4], Kyla Wilwayco[2,4], Elaine S Seto[6,7,8], Amita Sehgal[9,10], Shinya Yamamoto[1,2,4,5,11,*]

[1] Program in Developmental Biology, Baylor College of Medicine (BCM), Houston, TX 77030, USA

[2] Jan and Dan Duncan Neurological Research Institute (NRI), Texas Children's Hospital (TCH), Houston, TX 77030, USA

[3] Department of Neuroscience, University of Pennsylvania, Philadelphia, Pennsylvania, USA

[4] Department of Molecular and Human Genetics, BCM, Houston, TX 77030, USA

[5] Department of Neuroscience, BCM, Houston, TX 77030 USA

[6] Department of Neurology, TCH, Houston, TX 77030, USA

[7] Epilepsy Center, TCH, Houston, TX 77030, USA

[8] Department of Neurophysiology, TCH, Houston, TX 77030, USA

[9] Chronobiology and Sleep Institute, Perelman School of Medicine at the University of Pennsylvania, Philadelphia, PA, USA.

[10] Howard Hughes Medical Institute, University of Pennsylvania, Philadelphia, PA, USA

[11] Development, Disease Models & Therapeutics Graduate Program, BCM, Houston, TX 77030, USA

* Corresponding Author: Shinya Yamamoto

Correspondence: yamamoto@bcm.edu

Summary

The dopaminergic system has been extensively studied for its role in behavior and neurological diseases. Despite this, we still know little about how dopamine levels are regulated *in vivo*. To identify regulators of dopamine, we utilized *Drosophila melanogaster* cuticle pigmentation as a readout, where dopamine is used as a precursor to melanin. We started by measuring dopamine from known pigmentation mutants (e.g. *tan*, *ebony*, *black*) and then performed an RNAi-based screen to identify new regulators. We found 153 hits, which were enriched for developmental signaling pathways and mitochondria-associated proteins. From 35 prioritized candidates, 11 had an effect on head dopamine levels. Effects on brain dopamine were mild even when the rate-limiting synthesis enzyme *Tyrosine hydroxylase (TH)* was knocked down, suggesting changes in dopamine levels are tightly regulated in the nervous system. We pursued two of our hits that reduced brain dopamine levels, *clueless* and *mask*. Further examination suggests that *mask* regulates transcription of *TH* and affects dopamine-dependent sleep patterns. In summary, by studying genes that affect cuticle pigmentation, we were able to identify genes that affect dopamine metabolism as well as a novel regulator of behavior.

Keywords: *Drosophila melanogaster*, dopamine, pigmentation, RNAi, screen, *mask*, sleep

Introduction

Dopamine is a conserved neurotransmitter that functions in the nervous system to regulate a variety of behaviors, including learning & memory, locomotion, reward, and sleep. In humans, disruptions in dopamine have been associated with neurological and neuropsychiatric disorders, including addiction, depression, sleep disorders, and schizophrenia.[1–3] In addition, one of the hallmarks of Parkinson's disease is early degeneration of dopaminergic neurons, and Parkinson's patients are often given a dopamine precursor, l-dihydroxyphenylalanine (L-DOPA), as a method for treating symptoms.[4,5] Most genetic research on dopamine biology has focused on dopaminergic signaling and transport. However, changes in dopamine levels can have a great impact on behavioral outcomes.[6–8] Thus, identifying genes that affect dopamine levels is critical to understanding and potentially treating dopamine-associated disorders.

Dopamine synthesis is a conserved process, whereby the amino acid tyrosine is converted into L-DOPA via the rate-limiting enzyme, Tyrosine hydroxylase (TH).[9] Then, L-DOPA is converted into dopamine via the enzyme Dopa decarboxylase (Ddc).[10] In mammals, dopamine is degraded via oxidation or methylation using the enzymes Monoamine oxidase (MAO) and Catechol-O-methyltransferase (COMT).[11] In invertebrates, dopamine degradation goes through β-alanylation via the β-alanyl amine synthase (encoded by the *ebony* gene in *Drosophila melanogaster*) and acetylation via the acetyltransferase (encoded by the *speck* gene in *Drosophila*).[12] In addition, insects also convert dopamine into melanin to form proper cuticle pigment and structure. [13–15]For example, knockdown of *TH* (also known as *pale (ple)* in *Drosophila*) or *Ddc* leads to a paler cuticle, and reduction of *ebony* or *speck* leads to a darker cuticle.[13–15]

Historically, *Drosophila* has been used to study dopamine biology in multiple contexts. In particular, the fly has been instrumental in dissecting the role of dopamine in learning and

memory.[16,17] Moreover, an extensive genetic toolkit has made it a great model system for dissecting dopaminergic neural circuitry and signaling.[18–20] Lastly, *Drosophila* has been used to study dopamine-related neurological diseases. In particular, the fly was instrumental in identifying and investigating the cellular functions of Parkinson disease's genetic risk factors, *PINK1* and *PRKN* (i.e. *Pink1* and *parkin* in [21]*Drosophila*).[21]

As well as being a tool for dissecting neural circuitry, the fast generation time and low maintenance cost makes *Drosophila* a great system for large-scale screening. Previously, a RNAi screen (11,619 genes, ~89% of genome) was performed to identify genes that affect mechanosensory organs and cuticle formation in the *Drosophila* thorax.[22] In this screen, the researchers found 458 genes that affected cuticle color upon knockdown, but no further validation was performed.

Here, we utilize the fly cuticle to identify novel regulators of dopamine. We start by systematically examining classical pigmentation genes for their effect on dopamine in the head and brain. These experiments revealed that genes involved in dopamine synthesis cause the expected reduction in dopamine. On the other hand, genes involved in dopamine degradation either have no effect or unexpectedly show reduced dopamine. We go on to characterize 458 genes identified from the RNAi screen by Mummery-Widmer et al. (2009). We tested 330 of them with independent RNAi lines and validated 153 genes (~46%) with consistent cuticle pigmentation defects. We go on to examine 35 prioritized gene hits for their effect on dopamine levels. From this analysis, we found two genes, *mask* and *clu*, that reduced brain dopamine levels upon knockdown in dopaminergic neurons. Lastly, we used molecular biology and sleep behavioral studies to show that *mask* appears to alter brain dopamine through regulation of *TH* transcription.

Results

Drosophila pigmentation genes affect dopamine in unexpected ways

To systematically test if changes in pigmentation genes affect dopamine as theorized in the field, we characterized loss-of-function alleles of genes involved in dopamine metabolism (Figure 1A) for pigmentation phenotypes and dopamine levels. Since the enzymes required for dopamine synthesis (TH and Ddc) are essential for survival,[23,24] we took advantage of established RNAi lines and UAS/GAL4 system.[25–28] It is known that reduction of *TH* or *Ddc* causes pale pigmentation and reduced dopamine.[9,10,14] We validated our method by knocking down *TH* in the middle thorax using *pnr-GAL4* along with a verified RNAi,[29] which causes a strong pale cuticle phenotype (Figures 1B and 1C). We measured dopamine using HPLC, and in our hands, this RNAi reduces head dopamine levels by ~60% (Figure 1E) and brain dopamine levels by ~32% (Figure 1E'). *Ddc* knockdown causes a weaker effect than *TH* RNAi in the cuticle (Figures 1B and 1D) and the head (~35% dopamine reduction, Figure 1E) and has no significant effect on dopamine in the brain (Figure 1E'). This may be due to the strength of the RNAi and/or enzyme level requirements (since TH is the rate-limiting enzyme).

To test genes implicated in dopamine degradation and cuticle development (i.e. pigmentation and structural rigidity), we examined known mutant alleles. These alleles cause darker or paler cuticles (Figures 1F-1L and 1F'-1L') depending on their role in melanin metabolism. Unexpectedly, *black*, *speck*, *straw* and *yellow* mutants reduce head dopamine levels (measured using HPLC, Figure 1Q), while *ebony* and *tan* mutants had no significant effect (Figure 1Q). Next, we checked the brain expression patterns of pigmentation enzymes. Based on our own expression analysis (Figures 1M-1P) and previously reported expression data,[30,31] most are expressed in the fly brain, but their expression does not appear to overlap with DANs. None of these pigmentation gene mutations had a significant effect on brain dopamine (Figure 1R).

112 Together this data shows that changes in dopamine synthesis cause a paler cuticle, which
113 reflects a reduction in dopamine, but changes in dopamine metabolism enzymes downstream of
114 dopamine synthesis have pigmentation phenotypes that do not correlate with brain dopamine
115 level differences.

116 RNAi-based cuticle pigmentation screen

117 Mining a previously published genome-wide scale RNAi screen,[22] we identified 458 genes
118 with pigmentation defects. To check if these phenotypes can be reproduced, we located 718
119 additional UAS-RNAi lines corresponding to 330 genes. 426 lines came from the National Institute
120 of Genetics in Mishima, Japan,[32] and 292 came from the Transgenic RNAi Project (TRiP) at
121 Harvard Medical School.[25] 153 genes caused pigmentation defects in at least one additional RNAi
122 line, which validates the results for 46.4% of the previous screen's RNAi lines (VDRC collection,
123 Figure 2A).

124 Our RNAi-based secondary screen produced a spectrum of phenotypes (Figure 2B), but
125 the phenotypes strengths (mild, moderate, or strong) were equally represented (mild = 38%,
126 moderate = 33%, strong = 29%, Figure 2D). Pigmentation color changes were classified in three
127 primary categories, pale, dark, or mix (a combination of pale and dark in a single thorax), which
128 were not equally represented (Figure 2E). Dark cuticle phenotypes were the most common (56%),
129 with pale and mixed cuticle phenotypes seen in 28% and 16% of genes, respectively.

130 We performed a protein-network analysis (Figure 2C) and found a group of proteins
131 previously linked to cuticle pigmentation as well as clusters related to RNA processing, ubiquitin
132 proteasome system, mitochondria-associated proteins, and signaling pathway genes, Hippo and
133 EGF (epidermal growth factor) signaling in particular. GO enrichment analysis highlighted terms
134 associated with cuticle pigmentation, protein stability, and several signaling pathways (Figure S1).
135 We also observed that 85% of our genes were conserved between *Drosophila* and human, an

136 enrichment from the 68% of conserved genes in the original screen gene list (11, 619, Figures 2F
137 and S2).

138 In summary, the cuticle pigmentation screen identified a spectrum of pale, dark and mixed
139 phenotypes in 153 genes, showing a validation of ~50% from the original screen. Close
140 examination of these hits highlights conserved molecular processes.

141 Many pigmentation genes isolated have a neurological consequence

142 To investigate if our gene candidates have a neurological consequence, we first checked
143 if their homologs are associated with a neurological disease. Importantly, we defined homologs
144 or conserved genes as genes where an ortholog prediction algorithm (DRSC Integrative Ortholog
145 Prediction Tool) had a human gene with a score greater than or equal to three. We found that
146 51.2% of the fly gene homologs are associated with a disease, 78% of those have at least one
147 disease with neurological phenotypes (Table 1 and Figure S2), such as intellectual disability,
148 autism spectrum disorder, ataxia, epilepsy, and cerebral atrophy.

149 Since dopamine is known to regulate locomotion and sleep,[22,33] we screened for
150 locomotion and sleep defects using the Drosophila Activity Monitor (DAM).[34] We tested 274 RNAi
151 lines from the NIG, TRiP, and VDRC RNAi collections corresponding to the validated 153 gene
152 hits.[35–37] We scored the lines for total locomotion, total sleep, sleep bout length, and sleep latency
153 during the night and day (Figure 3). There was a broad range in the RNAi lines for each of these
154 phenotypes (Figure 3C). We classified RNAi lines as “outliers” if they were two standard
155 deviations from the mean for a given phenotype (locomotion: 23 lines, total sleep: 20 lines, sleep
156 bout length: 21 lines, sleep latency: 25 lines). While total sleep and locomotion strongly
157 overlapped with each other, sleep latency and sleep bout length did not overlap with the other
158 sleep phenotypes (Figure 3D). We assessed if certain gene categories (>10 genes) showed any
159 distinct behavioral patterns (Figure 2C). There was no change in total locomotion or total sleep in

160 the categories assessed (Figures 3F and 3G). However, each category showed a distinct pattern
161 in sleep bout length and latency (Figures 3F and 3H). This could indicate a distinction in how
162 different gene functions could affect sleep. Since genes that affect sleep can often show distinct
163 phenotypes (e.g. total sleep, bout number, latency, etc.) at distinct times of day,[38] any gene with
164 one phenotype during the day or night was classified as an "outlier". This produced 60 lines,
165 corresponding to 50 genes.

166 Taken together, 77 of our 132 conserved genes are likely to have a neurological function,
167 because they are implicated in human neurological disease (52 conserved genes) or were
168 classified as a behavioral "outlier" (45 conserved genes).

169 11 genes alter dopamine levels in the fly head

170 To prioritize our gene list for dopamine measurement, we classified which of our genes
171 were conserved in humans, as previously noted (132 conserved/153 pigmentation genes). Then,
172 we prioritized these based on whether knockdown of these genes showed a strong pigmentation
173 effect (38 genes), a behavioral effect in the DAM (45 genes), and/or a human neurological disease
174 association (52 genes). 72% (95/132 conserved genes) were represented in one of these
175 categories, and 29% (39/132) were represented in at least two (Figures 4A). We classified genes
176 in two or more categories as priority hits and tested them for changes in dopamine using High
177 Performance Liquid Chromatography (HPLC). We repeated previous results showing that
178 knocking down *TH* or overexpressing a *TH* cDNA using *TH-GAL4* significantly reduces or
179 increases head dopamine without effecting serotonin (Figures 4B and 4C).[29]

180 We found that 11 of 35 prioritized genes (note: some not tested due to lethality or stock
181 issues) significantly altered head dopamine levels (Figures 4D and 4E). Since control NIG lines
182 showed about ~80% dopamine levels compared to the TRiP collection (Figure S3), we compared
183 the DA levels to control lines appropriate for each collection (e.g. UAS-lacZ RNAi). Unlike cuticle

184 pigmentation, where 65% of genes caused a dark cuticle (excludes mixed cuticle phenotype),
185 most genes trended toward a reduction in dopamine (71%, 25/35, Figures 4F and 4G). There was
186 no correlation between the cuticle color and the dopamine level in the fly head (Figure 4H).

187 In summary, our HPLC analysis on fly heads revealed 11 genes that significantly affect
188 dopamine levels. We saw a trend in reduction in dopamine across all lines tested, and we
189 observed no correlation between cuticle color and dopamine level.

190 Brain studies reveal *mask* and *clueless* as regulators of brain dopamine

191 To determine which of the 11 gene hits have consequences in the brain, we examined if
192 their expression [39–41]overlapped with DANs. Looking at single-cell mRNA sequencing datasets,
193 we saw that 10 of our genes overlapped with some DANs (Figure S5), though the expression
194 overlap varied. *PIG-A* and *Sos* showed only ~3% overlap, and *Bsf* and *mask* showed 28% and
195 35% overlap with [42,43]DANs, respectively.[42,43] For five of our genes, we were able to examine their
196 expression using available T2A-GAL4 lines.[39–41] We found variability in the percentage of DANs
197 with overlapping expression, but three of them (*Bsg*, *ClC-c*, and *PIG-A*) overlapped with ~75% of
198 DANs, *rk* overlapped with ~45%, and mask overlapped with ~66% of the examined DAN clusters
199 (Figures S5, S6, 5A, 5B-D, and 5B'-D'). For *clu*, we were able to examine expression using a
200 protein trap line.[44,45] We saw that clueless protein appears to be enriched in DANs (Figures 5E,
201 5F-5H and 5F'-5H').

202 The *TH-GAL4* line commonly used for dopamine studies misses a large portion of DANs,
203 particularly in the PAM cluster (~87 DANs missed/~142 total DANs per hemisphere),[46] making it
204 not ideal for quantifying total changes in brain dopamine. We recombined the *TH-GAL4* with
205 another driver that hits a large portion of the PAM cluster neurons (*GMR58E02-GAL4 or R58-*
206 *GAL4)*[18] generating a recombined line (labelled *TH,R58-GAL4*) that hits ~95% of DANs (Figure
207 S4). We microdissected adult fly brains and measured dopamine for our 11 gene hits. Most of

208 them showed no change in brain dopamine (Figure S5), but *mask* (*multiple ankyrin repeats single*
209 *KH domain*) and *clueless* (*clueless*) knockdown reduced total brain dopamine for two independent
210 RNAi lines ([44,45]Figures 5I).

211 In summary, our fly brain analysis revealed that at least six (*Bsg*, *ClC-c*, *clueless*, *mask,*
212 *PIG-A*, *rk*) of our gene candidates show co-expression with TH, but only two genes (*clueless* and
213 *mask*) significantly altered brain dopamine upon knockdown in the majority of DANs.

214 *mask* regulates Tyrosine Hydroxylase and alters sleep in a dopamine-
215 dependent manner.

216 To test if *clu* and *mask* knockdown could be due to DAN loss, we quantified the number
217 of DANs in several clusters.[46] There was no difference in neuron number for any cluster examined
218 (Figures 5L and S6). Since our pigmentation gene study revealed that only the manipulation in
219 TH reduced brain dopamine (Figure 1), we examined if knocking down our genes affect TH.
220 Knockdown of *mask* led to a significant reduction in *TH* mRNA level for one RNAi (50% reduction),
221 with the other RNAi trending (20-30% reduction, Figure 5J). Upon examining TH protein levels in
222 DAN clusters, two clusters showed significant reduction in TH protein level, with other clusters
223 showing a trend in TH protein reduction (PAL and PPM2/3, Figures 5K and S6). To assess
224 behavioral consequences, we performed additional sleep analysis on *mask*. Dopamine is a wake-
225 promoting agent, and complete loss of dopamine in the brain significantly increases sleep.[47,48]
226 Knocking down *TH* using the *TH-GAL4* did not significantly alter total levels of sleep during light
227 or dark periods (Figure S7), which may be due to the selective expression of the GAL4 or the
228 partial reduction of dopamine (Figure 4C). However, two hours before light onset, there was a
229 significant increase in sleep, accompanied by a reduction in the locomotor activity that anticipates
230 light . Similarly, knockdown of *mask* with the TH-GAL4 showed a highly consistent reduction in
231 light anticipation (Figures 6A, 6B, 6B', and S8). When we feed the flies L-DOPA, the effect is no

232 longer seen (Figures 6C and S8). Additionally, in *Drosophila* caffeine's effects on sleep are
233 mediated by dopamine through a point that is upstream of L-DOPA.[49] Based on this, we suspected
234 that *mask* knockdown would ameliorate the effects of caffeine on sleep, since *mask* appears to
235 reduce the synthesis of *TH*. We saw that caffeine's effect on total sleep and sleep in the dark is
236 ameliorated upon *mask* knockdown (Figures 6D, 6E, and S8).

237 Follow up studies on *clueless* showed that *clueless* knockdown increases TH RNA level
238 by about 1.5-2X, with no effect on TH protein level or TH+ neurons (Figure S9), and while there
239 was an increase in sleep across several RNAi lines, there is no light anticipation phenotype.
240 Feeding *TH>clu RNAi* flies L-DOPA was unable to rescue the *clueless* effects on sleep (Figure
241 S9), suggesting that the effects on dopamine and TH may be a secondary effect. Additionally, the
242 antioxidant NACA was also unable to rescue the sleep defects seen upon *clueless* knockdown
243 (Figure S9).

244 In conclusion, *mask* appears to reduce total dopamine levels and sleep by affecting
245 transcription of *TH*, while *clueless* is acting through an alternative mechanism.

246 Discussion

247 Validation of 148 novel cuticle pigmentation genes

248 Our RNAi screened confirmed 153 genes that were previously implicated in *Drosophila*
249 pigmentation – 148 of these genes have not been previously associated with dopamine biology.
250 Since we observed a strong enrichment for genes involved in pigmentation and tyrosine
251 metabolism (Figure S1), our screening method effectively identified genes that are involved in the
252 process of interest.

253 While prior research has compared genes that overlap with different types of screening
254 strategies (e.g. chemical mutagenesis vs. RNAi), most RNAi phenotypes from large-scale screens
255 have not been validated with alternative RNAi lines or collections. The original source RNAi
256 screen used the lines available at the VDRC stock center.[35,37] Alternative sources for RNAi lines
257 (i.e. TRiP and NIG) start with different backgrounds, vectors, hairpin lengths, insertion methods,
258 and/or target different areas of the gene.[36,50] This allows researchers to overcome the off-targeting
259 and weak silencing seen with RNAi analysis, but to our knowledge, there have been no screens
260 or meta-analyses to test consistency from different lines. In this study, we found that ~46.4%
261 (153/330) of genes with a pigmentation phenotype showed a phenotype in an alternative RNAi,
262 and 87% of those phenotypes showed agreement in pigmentation color, highlighting that
263 pigmentation as a phenotype is relatively consistent (Figure S10).

264 Interestingly, 85% of our genes had a homolog, whereas the original RNAi screen list
265 (11,619 genes) had 68% of genes with a homology (1.25-fold enrichment, Figure S2). This is
266 striking since dopamine cuticle pigmentation is an invertebrate-specific phenomenon,[12] and the
267 enrichment suggests this phenotype is relevant for a conserved biological pathway. We propose
268 that cuticle pigmentation may be a "phenolog" [51]of certain neurological traits in mammals.[51]

269 Protein-protein interaction network highlights unexpected gene associations

270 When we investigated what kind of gene categories were found in the pigmentation
271 screen, we saw clusters that are associated with ubiquitin-proteasome system (UPS), RNA
272 processing, mitochondria, and developmental signaling pathways. Each of these processes could
273 be relevant to dopamine biology. For example, there is some evidence that the UPS system
274 regulates TH levels in the mammals since inhibition of the UPS system has been shown to
275 increase the TH protein in a PC12 rat cell line.[52,53] In addition, changes in RNA processing could
276 indicate changes in the dopamine synthesis enzymes TH and Ddc since these enzymes undergo

277 RNA processing to create two different isoforms.[54] The TH isoforms differ in tissue expression
278 and kinetics.[55] In mammals, post-transcriptional trafficking of TH mRNA and translational
279 regulation has been suggested to be important for its function.[56]

280 We identified 12 genes that are known to function at the mitochondria, mostly in the
281 electron transport chain (*ND-13B*, *ND-42*, *COX5A*), mitochondrial mRNA translation (*mRpL47*,
282 *mRpL48*, *CG4679*), and mitochondrial protein localization (*CG8728*, *clu*, *mask*, *Mpcp2*). It is well-
283 known that the mitochondria have a key role in dopamine metabolism in mammals since MAO
284 acts in the mitochondria to degrade dopamine. However, there is no known MOA homolog in
285 flies.[12] The metabolites for oxidation and methylation of dopamine (DOPAC and HVA) have been
286 observed in flies though,[57–60] and we saw that dopamine degradation enzyme mutants (*ebony*,
287 *tan*, and *speck*)[61,62] had no effect on dopamine in the brain (Figure 1). It is possible that there is
288 an alternative process that regulates dopamine degradation in the brain, and the mitochondria
289 may be involved.

290 The last major group of genes identified from our screen was developmental signaling,
291 specifically EGF signaling and Hippo signaling. To date, neither EGF nor Hippo signaling have an
292 established connection with dopamine biology in *Drosophila*. We may have pulled these genes
293 out is because forming the dorso-central thorax is developmentally regulated.[63–65] However, we
294 did not identify core components of the other key pathways, such as Notch or Hedgehog,
295 suggesting that EGF and Hippo are more specifically involved in this pigmentation process.

296 Cuticle pigmentation phenotypes may not reflect changes in dopamine

297 The field has generally assumed that a darker cuticle reflects an elevated level of
298 dopamine.[15,66] However, when we measured dopamine from degradation enzyme mutants using
299 HPLC, we saw either no effect on dopamine level or reduced level of dopamine in the head. In
300 addition, when we measured dopamine from the pigmentation genes from the screen, a darker

301 cuticle did not reflect elevated levels of dopamine in the head. While we were able to increase
302 dopamine by 3-5 fold upon TH cDNA overexpression in the head (Figure 4C), this phenomenon
303 was not observable in the brain. One reason could be that there is a selective pressure or a strong
304 feedback mechanism that prevents elevated levels of dopamine in the nervous system. Since
305 oxidized dopamine could be toxic,[67] this could be a mechanism to prevent cell toxicity.
306 Regardless, changes in cuticle pigmentation do not necessarily reflect changes in dopamine level.

307 Upon seeing alterations of dopamine in the head for some of the classic pigmentation
308 genes, we tested if this corresponded to changes in the brain. In the case of established dopamine
309 synthesis genes, we saw a mild reduction in dopamine (~25%) upon knockdown of the rate-
310 limiting enzyme, *TH*, and no effect upon knockdown of *Ddc*. In addition, we saw no effect on brain
311 dopamine from dopamine degradation enzymes. Taken together, this suggests that brain
312 dopamine is under very tight regulation, and effects on the enzymes may be difficult to see in total
313 dopamine level. It also highlights how our approach will likely miss relevant candidates. In
314 addition, upon looking at expression in the brain of dopamine degradation enzymes, we saw they
315 did not overlap well with DANs. It may be that dopamine degradation does not happen in the
316 neurons since it was hypothesized to occur in the glia.[31,68] However, the expression does not
317 match a broad glial expression either. For the 11 genes from the pigmentation RNAi screen that
318 showed altered levels of dopamine, only 2 (18%) of them showed an effect on dopamine in the
319 brain. These results highlight how head dopamine levels should not be used as a proxy for brain
320 dopamine levels.

321 *clu* and *mask* reduce brain dopamine levels through different mechanisms

322 Once we identified that knockdown of *clueless* and *mask* both reduced dopamine in the
323 brain without affecting the number of DANs, we hypothesized that they may be acting through

324 TH. This is primarily because our initial dopamine metabolism studies showed that only changes
325 in TH significantly affected dopamine levels in the brain.

326 *mask* encodes a scaffolding molecule that functions in multiple contexts.[69–71] In this study,
327 *mask* knockdown reduced *TH* mRNA and protein levels, suggesting it acts on TH transcription.
328 Follow-up behavior analysis showed that *mask* knockdown in DANs led to a highly consistent
329 change in sleep. Specifically, *mask* knockdown reduced the number of flies that anticipated light.
330 While fruit flies typically start to wake before light onset,[72] loss of mask in DANs suppresses this
331 anticipation behavior. Importantly, dopamine has a role in sleep that goes beyond light
332 anticipation, and complete loss of dopamine causes a global increase in sleep in the day and
333 night.[73] The phenotype we observe is not this severe, which may be due to the GAL4 driver not
334 hitting all DANs or the fact that this knockdown is only reducing dopamine by a modest 15-20%
335 (Figure 5). This is supported by the similar phenotype with the TH RNAi and the DAN driver
336 (TH>TH RNAi, Figure S7). There may be a circadian component as well. It is plausible that
337 dopamine synthesis increases before wake at light onset, and manipulations that affect TH levels
338 may struggle to keep up with the dopamine synthesis required at this time of day.

339 When we fed *mask* knockdown flies the precursor for dopamine, L-DOPA, this abolished
340 the effect on light anticipation. We suspect that feeding L-DOPA does not override all sleep-
341 dependent effects because clueless sleep phenotypes remained when we fed them L-DOPA
342 (Figure S9). There is evidence that in the fruit fly caffeine affects sleep through TH. Specifically,
343 Nall et al. showed that caffeine's effect on sleep is absent in TH mutant flies, even if L-DOPA is
344 given.[49] Since *mask* knockdown affects TH mRNA levels, we tested if mask knockdown would
345 suppress the effects of caffeine. We found that the reduction in total sleep and sleep during the
346 dark period normally seen upon caffeine administration were absent upon mask knockdown. This
347 further supports that mask alters TH levels.

348 While we do not have any direct evidence for how *mask* may be altering TH levels, *mask*
349 has been implicated in multiple biological pathways that were highlighted from our screen,
350 including EGF signaling (e.g. *Egfr*, *Sev*, Raf), Hippo signaling (e.g. *hpo*, *wts*, *mats*), and
351 mitochondrial biology.[74–77]. Egf and Hippo signaling have well-known transcriptional effects,[78,79]
352 but whether they may regulate TH transcription directly or indirectly in this context need further
353 investigation. It is also possible that *mask* is acting in several of these pathways at once, which
354 causes it to have a strong additive effect that produces a significant change in dopamine in the
355 whole brain, while knockdown of individual pathways may have more restricted roles (e.g. *Egfr*,
356 *Sos*, *hpo*).

357 In addition to *mask*, we also saw that knockdown of *clueless* leads to significant reduction
358 in dopamine. However, when we explored the behavioral consequence of *clueless* knockdown, it
359 did not show the same effect on sleep as *mask* or *TH* knockdown. In addition, the sleep phenotype
360 was not rescued by L-DOPA, and molecular biology showed that *clueless* knockdown leads to an
361 increase in TH mRNA with no change in TH protein. Taken together, this indicates that the effect
362 on dopamine from *clueless* knockdown may be a secondary consequence. *clueless* encodes a
363 ribonucleoprotein thought to act at the outer mitochondrial membrane to promote proper formation
364 of protein complexes including mitophagy proteins like Pink1 and Parkin.[80,81] It also interacts with
365 the ribosome and translocase complex at the mitochondrial membrane suggesting it acts as a
366 regulator for mitochondrial protein translation and import. [80,82] Knockdown of *clueless* showed no
367 effect on TH protein level, but since this is a mitochondrial protein, it may be more likely that the
368 effect on dopamine is through the previously proposed roles of mitochondria in regulating
369 dopamine levels.

370 Importantly, our analysis has focused on changes in dopamine caused by changes in
371 synthesis or degradation. However, dopamine levels can also be regulated by changes dopamine
372 trafficking through regulators like the dopamine transporter (DAT) or the vesicular monoamine

373 transporter (VMAT).[12] For example, a null allele of the *DAT, fumin*, causes elevated levels of
374 dopamine that lead to behavioral phenotypes, including hyperactivity and reduction in sleep.[48]
375 However, these mutants do not have any cuticle pigmentation defects. While the role of VMAT in
376 cuticle pigmentation have not been investigated, whether dopamine secretion from the epithelial
377 cells remains a mystery. Therefore, it would be important to further study whether some of the
378 hits from our screen may affect dopamine levels through altering dopamine transport via
379 regulating DAT, VMAT or other mechanisms that regulates dopamine dynamics.

380 Some regulators of dopamine levels may act locally

381 When we examined the expression of some of our pigmentation genes in the brain (Figure
382 S11), we found that many of them do not overlap with all DANs. This indicates that measuring
383 global changes in dopamine may not be best for determining effects on DA for many of these
384 genes. They may require targeted dopamine measurements, perhaps through a fixed or live
385 reporter.[83,84] It is also possible to assess changes in dopamine using behavior, but this would
386 require detailed assessment for each gene since behaviors are often cluster specific.[85]

387 In conclusion, our screen of identified novel pigmentation genes, a subset of which were
388 identified as novel regulators of dopamine *in vivo*. Unbiased forward genetic screens in model
389 organisms are powerful ways to identify unanticipated links between distinct biological pathways
390 and provide new molecular handles to study the functional connections between them. Application
391 of such strategies to the regulation of dopamine levels will likely continue to identify novel factors,
392 some of which will impact our understanding of human neurological and neurodevelopmental
393 diseases.

394 Limitations of the study

395 One key limitation to this study is that this screening approach will not capture all
396 regulators of dopamine in the brain. The screen and most of the experiments are based off of
397 RNAi lines. These lines were not verified for the initial and secondary screens. Some RNAis may
398 not work. In addition, the RNAis often do not have the same effect as full mutants. For example,
399 the TH RNAi, which has a known large effect on TH mRNA level (~90% reduction) still only
400 reduces dopamine by ~30% in the brain. However, the full mutant for TH removes all dopamine
401 from the brain. In addition to this the initial screen was based on pigmentation, and if a gene that
402 regulates dopamine in the brain is not expressed in the cuticle, it would not have been captured.
403 Our secondary screening uses total dopamine levels in the head and brain. It is likely that mild or
404 cell-type specific changes in dopamine would not be captured through this approach. When we
405 examined *clu* and *mask*, we focused on regulation through the dopamine synthesis enzymes.
406 There are many ways that *clu* and *mask* could regulate dopamine, including through genes such
407 as VMAT and DAT. We cannot rule out dopamine regulation through these alternative
408 mechanisms.

409 Resource Availability

410 All data generated or analyzed during this study are included in this published article and its
411 supplementary information files. This study did not generate any new unique reagents.

412 Acknowledgements

413 We thank the Bloomington *Drosophila* Stock Center (USA), the National Institutes Genetics Fly
414 Stock Center (Japan), *Vienna* Drosophila RNAi Center (Austria) and Dr. Hugo Bellen for providing
415 useful fly stocks and reagents for this project. We would like to thank Drs. Jonathan Andrews,
416 Hugo Bellen, Brigitte Dauwalder, Herman Dierick, Linsday Goodman, Oguz Kanca, Kartik
417 Venkatachalam, Michael Wangler, Sheng Zhang, Huda Zoghbi, and the Sehgal lab for useful

suggestions, discussions and advice on the project. This work was supported by startup funds to Dr. Shinya Yamamoto from the Jan and Dan Duncan Neurological Research Institute at Texas Children's Hospital and the Department of Molecular and Human Genetics at Baylor College of Medicine, by the IRACDA program at the University of Pennsylvania (K12GM081259) for Dr. Samantha Deal, and by Howard Huges Medical Institute (HHMI) for Dr. Amita Sehgal. Confocal microscopy at BCM was supported in part by the Intellectual and Developmental Disabilities Research Center (IDDRC, U54HD083092) from the Eunice Kennedy Shriver National Institute of Child Health & Human Development.

Authors Contributions

S.Y., E.S.S., A.S., and S.L.D. conceived the experiments. S.Y. and S.L.D. wrote the manuscript. S.Y., E.S.S., D.B., and S.L.D. conducted the pigmentation screen and DAM behavior analysis screen. S.L.D. and K.W. conducted the pigmentation mutant analysis experiments. S.L.D., S.B.G, H.D-S, Y.F., and K.W. conduced the HPLC analysis. S.L.D. and Y.F. performed confocal imaging. S.L.D. conducted all data analysis. All authors participated in the critical analysis of the manuscript.

Declarations of Interests

The authors declare no competing interests.

Figure Titles and Legends

Figure 1. Manipulation of pigmentation enzymes have unexpected effects on dopamine. (A) *Drosophila* dopamine metabolism pathway. Gene names encoding pigmentation enzymes are in blue and metabolites are in black. (B-D) Thorax phenotypes observed upon knockdown of

439 Tyrosine hydroxylase (TH, also known as Pale) (C) and Dopa decarboxylase (Ddc) (D) compared
440 to control (B). (E-E') Dopamine levels, measured using HPLC, from the heads (E) and brains (E')
441 upon knockdown of *TH* and *Ddc*. Pigmentation phenotypes observed mutant alleles in the thorax
442 (F-L) and the body (F'-L') (Arrow in I' indicates the darker region characteristic of *speck* mutants).
443 *T2A-GAL4* alleles for *black*, *speck*, and *tan* adult brain expression with dopaminergic neurons
444 (DAN) staining in magenta (DANs) (M-P). (Q) Dopamine, measured using HPLC, in the heads of
445 classical pigmentation mutants, $black^1$, $ebony^1$, $straw^1$, and $yellow^1$. (R) Dopamine levels in
446 dissected brains of classical pigmentation mutants. Ordinary one-way ANOVA test with Dunlett
447 multiple comparisons test. *=p<0.05, **=p<0.01, ***=p<0.001, ****=p<0.0001. Error bars show
448 standard deviation (SD).

449 **Figure 2. RNAi pigmentation screen reveals a broad spectrum of phenotypes and classes**
450 **of genes** (A) Flow chart depicting screening process. (B) Examples of the phenotypes observed
451 from the RNAi-based pigmentation screen. (C) Protein-protein interaction network for 153 high
452 confidence pigmentation gene hits from the RNAi-screen using STRING network analysis.
453 Strength of line indicates confidence or strength of data support. Genes with no known
454 interactions are not displayed. (D-F) Pie charts for the 153 pigmentation gene hits, including
455 strength of phenotype (D), phenotype color (E), and conservation (F).

456 **Figure 3. *Drosophila* Activity Monitor (DAM) screen identifies behavior "outliers" and**
457 **highlights distinct phenotypes for gene categories.** (A-B) Representative activity and sleep
458 data measured in a neutral RNAi line (*mCherry RNAi*, A) and a behavioral "outlier" (*Raf RNAi*,
459 B) knocked down in DANs (*TH-GAL4*). (C) Bar graph showing all RNAi lines tested for 24hr
460 locomotion and total sleep during the 12hr light period, where light pink/blue represents fly lines
461 ±1SD away from the mean, and dark pink/blue are fly lines ±2SDs away from the mean (a.k.a.
462 "outliers"). (D) Venn diagram of "outliers" for the four phenotypes examined (sleep latency, sleep
463 bout length, locomotion, and total sleep). (E-H) Behavioral analysis of lines in three gene

464 categories captured in the pigmentation screen, including locomotion (E), sleep latency (F),
465 sleep bout duration (G), and total sleep (H). Individual t-tests were performed to assess if genes
466 in a category were significantly different to all other genes tested, and only those with a $p<0.10$
467 are reported, with *=$p<0.05$.

468 **Figure 4. Eleven genes alter head dopamine upon knockdown.** (A) Venn diagram of the
469 categories used to prioritize 39 genes (in yellow). (B) Representative chromatograms for
470 dopamine (DA) and serotonin (5-HT) upon knockdown or overexpression of TH in Dopaminergic
471 cells (*TH-GAL4*). (C) Quantification of DA and 5-HT from chromatograms. (D-E) HPLC analysis
472 on prioritized genes for UAS-RNAi lines from NIG (D) and TRiP (E). (F-G) Pie charts for all
473 genes for cuticle color (F) and trend in dopamine (G). (H) XY plot comparing pigmentation
474 phenotype to dopamine levels. For (C) Brown-Forsythe ANOVA test performed with Dunnett's
475 T3 multiple comparisons test. For (D) and (E) ordinary One-way ANOVA test with Dunnett's
476 multiple comparisons test. **=$p<0.01$, ***=$p<0.001$, ****=$p<0.0001$. Error bars represent SD.

477 **Figure 5. Brain dopamine analysis identifies *mask* and *clu* as novel regulators of**
478 **dopamine levels in the fly brain** (A) *mask^{T2A}>mCh::nls* (represented as green) expression
479 pattern in the adult brain colabelled with a TH antibody staining DANs (magenta), with specific
480 clusters shown (B-D, B'-D'). (E) *clu::GFP* expression pattern in the adult brain colabelled with
481 TH (magenta), with specific clusters shown (F-H, F'-H'). (I) Total dopamine in the adult fly brain
482 upon knockdown of *mask* and *clu*. (J) qRT-PCR of TH upon *mask* knockdown with the
483 recombined DAN (*TH, R58-GAL4*) driver. (K) Quantification of total TH protein level through
484 immunofluorescence in DAN clusters upon knockdown of *mask*. (L) Quantification of TH positive
485 (TH+) neurons in DAN clusters upon knockdown of *mask*. Ordinary one-way ANOVA was done
486 with Dunnett's multiple comparisons test (I-L). Error bars represent SD. Scale bars are 50 μm in
487 (A) and (E) and 10 μm in all others. Closed arrowheads represent some cells with coexpression

488 between *mask*^{T2A}*>mCh::nls* and TH. Open arrowheads represent cells with TH staining and no
489 *mask*^{T2A}*>mCh::nls* expression.

490 **Figure 6. *mask* knockdown reduces TH mRNA and protein and causes sleep phenotypes**
491 **that align with reduction in TH levels** (A) 24-hr sleep graph (sleep binned in 30-minute
492 intervals) upon mask knockdown using the TH-GAL4. (B) Quantification of total sleep
493 throughout the 12-hr dark period upon mask knockdown (B') Quantification of light anticipation
494 upon mask knockdown. (C) Light anticipation in mask knockdown flies with L-DOPA feeding. (D-
495 E) Caffeine effects on sleep upon mask knockdown – (D) Total Sleep and (E) Sleep during the
496 12-hr dark period. For samples with more than one experimental, ordinary one-way ANOVAs
497 were performed with Dunnett's multiple comparisons. (B, B', C). For samples with one
498 experimental, individual t-tests were performed (D,E). *=p<0.05, **p<0.01, ****p<0.0001. Error
499 bars represent SD.

500 # Tables

501 **Table 1. Fly pigmentation genes identified from this screen with neurological disease**
502 **associated homologs in human.**

Fly Gene	Human Homologs with Neurological Phenotypes (DIOPT Score, Max=18)	Notable Neurological Phenotypes
AP-1sigma	AP1S2 (12), AP1S1 (11), AP2S1 (3)	ataxia, DD, seizures
ATP7	ATP7A (13), ATP7B (13)	dystonia, neurodegeneration, seizures, tremor
Atu	LEO1 (10)	ASD
byn	TBXT (11), TBX19 (10)	neural tube defects, seizures
CG16758	PNP (14)	ataxia, behavioral problems, spastic diplegia, tremor
CG4328	LMX1B (10)	spina bifida
CG43689	MYT1L (7)	DD, ID

CG4679	PTCD3 (14)	cerebral atrophy, myoclonus, psychomotor delay
CG5902	AAMERCR1 (13)	cerebral atrophy, early motor delay, myoclonus
CG8728	PMPCA (15)	ataxia
ClC-c	CLCN3 (12), CLCN4 (11), CLCNKA (3)	ID, language delay, seizures, structural abnormalities
ctrip	TRIP12 (10)	delayed speech, ID, psychomotor delay
Cyp301a1	CYP24A1 (5), CYP27B1 (4), CYP27A1 (4)	ataxia, motor delay, psychiatric symptoms, seizures
CysRS-m	CARS2 (15)	cerebral atrophy, epilepsy, psychomotor delay
Ddc	DDC (14), HDC (4)	dystonia, psychomotor delay, sleep disturbance
Dgp-1	GTPBP2 (3)	ataxia, dystonia, ID, psychomotor delay, seizures
Dscam2	DSCAM (10)	ASD
Egfr	ERBB4 (10), ERBB2 (10), ERBB3 (9)	ALS, axonal neuropathy, DD, seizures
Gbeta13F	GNB1 (15), GNB4 (13), GNB2 (12), GNB5 (3)	ADHD, CMT, DD, ID, language delay
gig	TSC2 (13)	brain structural abnormalities, seizures
Hrb98DE	HNRNPA2B1 (12), HNRNPA1 (9)	ALS, dementia, motor neuropathy
Itpr	ITPR1 (14), ITPR3 (11)	ataxia, cerebellar atrophy, motor delay
Khc	KIF5C (12), KIF5A (12)	ALS, psychomotor delay, seizures, spastic paraplegia
Larp7	LARP7 (10)	anxiety, DD, ID, unstable gait
LeuRS-m	LARS2 (15)	cognitive impairment, DD, dystonia, tremor, seizures
mask	ANKRD17 (10)	DD, ID, motor delay, speech delay
mbt	PAK1 (3), PAK3 (3), PAK2 (3)	ID, macrocephaly, seizures, speech delay
Membrin	GOSR2 (13)	cerebral atrophy, DD, seizures
Mp	COL18A1 (6)	ataxia, seizures

Mpcp2	SLC25A3 (14)	motor delay
ND-13B	NDUFA5 (13)	ASD
ND-42	NDUFA10 (14)	DD, strutural abnormalities
Npc2b	NPC2 (7)	behavioral problems, DD, dementia, dystonia, seizures
per	PER3 (8), PER2 (7)	sleep abnormalities
PIG-A	PIGA (15)	seizures, structural abnormalities
ple	TH (15)	ataxia, dystonia, Parkinsonism, motor and sleep delay
Prosap	SHANK2 (10), SHANK3 (8)	ASD, DD, schizophrenia, seizures
Raf	BRAF (14), RAF1 (11)	DD, seizures
Rbp9	ELAVL2 (12), ELAVL3 (10)	ASD
rdx	SPOP (10)	DD, ID, speech delay
robo1	ROBO3 (8)	structural abnormalities
SCOT	OXCT1 (15)	coma, psychomotor delay
sesB	SLC25A4 (12)	motor delay, hyperreflexia
slp1	FOXG1 (6), FOXI1 (3), FOXJ1 (3), FOXC1 (3)	dystonia, motor delay, sleep and structural abnormalities
Smurf	ITCH (4), NEDD4L (3)	ID, psychomotor delay, seizures
Sod3	SOD1 (4)	ALS, spastic tetraplegia
Sos	SOS1 (14), SOS2 (12)	cognitive impair, learning disabilities
Spn38F	SERPINC1 (4), SERPINI1 (4)	cerebral atrophy, dementia, seizures
stv	BAG3 (9)	abnormal gait, behavioral problems, neuropathy
tws	PPP2R2A (13)	ataxia
Usp2	USP8 (4)	behavioral problems

Usp7	USP7 (13)	ID, psychomotor delay, seizures, structural abnormalities

503

504 **Table 1.** Homologs were defined as a Drosophila Integrative Orthology Prediction Tool (DIOPT,
505 version 8.0) score greater than or equal to three. Neurological disease associations were based
506 on Online Mendelian Inheritance in Man (OMIM)_clincal disease phenotypes and high-confident
507 ASD genes listed in Simons Foundation Autism Research Initiative (SFARI) gene database (class
508 S, 1, 2 or 3). ASD=Autism Spectrum Disorder, DD=Developmental Delay, ID=Intellectual
509 Disability, ALS=Amytrophic Lateral Sclerosis, CMT=Charcot-Marie-Tooth disease.

510 STAR★Methods

511 Experimental Model and Study Participant Details

512 Fly Maintenance and Stocks

513 Flies (*Drosophila melanogaster*) were reared at 25°C on a 12:12 Light/Dark (LD) and fed a
514 molasses-based food source unless otherwise specific. Different temperatures were used to
515 achieve different levels of gene knockdown or overexpression, which is documented for each
516 experiment. Flies were transferred to a new vial 0-2 days post-eclosion (dpe) for age-appropriate
517 analysis. Experiments were run on 3-7 dpe flies unless otherwise stated. Mutant and transgenic
518 trains were obtained from Bloomington *Drosophila* Stock Center (BDSC,
519 https://bdsc.indiana.edu/), Vienna Drosophila Research Center (VDRC,
520 https://www.viennabiocenter.org/vbcf/vienna-drosophila-resource-center/), the Japanese
521 National Institute of Genetics (https://shigen.nig.ac.jp/fly/nigfly/), or were gifts from scientists in
522 the field or generated in house (S1 Table – S5 Table).

523 Fly Crosses

524 For the cuticle screen, *pnr-GAL4*[86] was crossed to the specified UAS-RNAi line (see S1 Table) at
525 29°C, 25°C, and/or 18°C and examined after pigmentation is completed (>1 dpe). For the
526 behavior and HPLC analysis *TH-GAL4* females (also called *ple-GAL4*, BDSC stock #8848) were
527 crossed to the specified RNAi line (see S2 Table). For all HPLC analysis, the controls were
528 specific to the tested UAS-RNAi line.[87] Thus, the TRiP collection of RNAi lines are compared to
529 the *UAS-mCherry(mCh) RNAi* line (BDSC #35785) and the NIG collection of RNAi lines as well
530 as the VDRC RNAi lines are compared to the *UAS-lacZ RNAi* line. For the HPLC analysis
531 performed on brains, we recombined the *TH-GAL4* with another DAN driver *GMR58E02-GAL4*
532 (BDSC #41347), which expresses in a large group DANs in the PAM cluster.[27] These flies are
533 referred to as *TH,R58-GAL4* throughout the article. The *TH,R58-GAL4* line was also used for
534 qPCR and TH protein analysis via immunohistochemistry. For gene expression analysis *UAS-*
535 *mCh::nls* (BDSC #38424) females were collected and crossed with respective T2A-GAL4 lines
536 (see S5 Table). Female and males were both imaged at ~5-7dpe. For the follow-up sleep studies,
537 the *UAS-RNAi* males were crossed with *TH-GAL4* virgins for the experimental. For the controls
538 w^{1118} females were crossed to males from either the *TH-GAL4* and *UAS-RNAi* lines
539 independently.

540 Method Details

541 Notum Dissection and Imaging

542 For thorax analysis and dissection, males and females were both selected, though differences
543 were not generally observed, and females are shown here. Flies that were 3-5 dpe were collected
544 and placed in 70% EtOH. Notum dissection and imaging was previously published.[88] In summary,
545 the thorax was dissected by removing the legs, abdomen, and head. Then the thorax was cut
546 such that a hole was on the ventral side to allow solution to pass into the thorax. These dissected
547 thoraces were placed in 10% KOH for 10 minutes at 90°C on a heat block. Then, the KOH was

548 removed and replaced with 70% EtOH solution. They were mounted on a slide prepared with tape
549 on two sides in mounting media (50% glycerol, 50% EtOH). The thoraces were imaged on a
550 stereo microscope (Leica MZ16) using OPTRONICS® MicroFIRE camera. The images are z-
551 stack brightfield images taken and collapsed using extended depth of field in Image-Pro Plus 7.0
552 and In-Focus (Version 1.6).

553 ## Brain Expression Analysis

554 Brain dissections and imaging were performed as previously reported.[89] In summary, the brains
555 were dissected at 3-7 dpe in ice cold PBS and then fixed in 4% PFA in 0.5% PBST for 20 minutes.
556 Then, they were washed with a quick wash in 0.5% PBST followed by three 10-20-minute washes
557 in 0.5% PBST while on a rotator. The samples were placed in primary antibody solution [anti-
558 Tyrosine Hydroxylase 1:500, PelFreez Biologicals, rabbit, P40101; anti-elav 1:100,
559 Developmental Studies Hybridoma Bank, rat, 7E8A10 in solution (5% Normal Donkey Serum,
560 0.1% NaN_3 in 0.5% PBST)] at 4°C for 3 days. Then, the samples were washed with a quick wash
561 in 0.5% PBST followed by three 10-20-minute washes in 0.5% PBST while on a rotator. After the
562 last wash, the samples were placed in a secondary antibody solution [anti-Rabbit 1:200 (Thermo
563 Fisher Sci., Alexa-647, A-21208); anti-rat 1:200 (Thermo Fisher Sci., Alexa-488, A-27040) in
564 solution (5% Normal Donkey Serum, 0.1% NaN_3 in 0.5% PBST)] for two hours at room
565 temperature. The samples were washed again with one quick wash followed by three 10-20
566 minutes washes in 0.5% PBST on a rotator. Then, the brains were mounted in Vectashield
567 mounting media and imaged on a confocal microscope (Zeiss LSM 710 or Zeiss LSM 880). All
568 images shown in this manuscript are Z-projection images that were generated using the ZEN
569 software (Zeiss). Quantification of co-expression with DANs and the T2A-GAL4 lines was done
570 by counting how many individual TH+ neurons for each cluster had a cell body labeled by the
571 *T2A-GAL4>mCherry::nls* signal. This quantification was done per hemisphere. The single cell

572 sequencing expression analysis was done based on the DAN cluster from adult fruit fly data found
573 in the Fly Cell Atlas, specifically using the data from Davie, Jannssens and Koldere et al., 2018.[91]

574 RNAi-based Pigmentation Screen

575 We identified pigmentation gene hits from a primary screen performed in Jurgen Knoblich's lab
576 using the Vienna Drosophila Resource Center collection of RNAi lines by accessing their public
577 RNAi screen database (https://bristlescreen.imba.oeaw.ac.at/start.php). The original screen was
578 performed on 20,262 RNAi lines, encompassing 11,619 genes (~82% of protein-coding genes).[22]
579 We selected genes that showed a cuticle pigmentation score for any RNAi line tested (gene
580 scores ranged from two to ten). To validate pigmentation defects, we selected genes that had
581 RNAi lines within the Fly National Institute of Genetics (NIG, 220 genes, 426 RNAi lines) or the
582 Harvard Transgenic RNAi Project (TRiP, 221 genes, 292 RNAi lines) collections. Each RNAi line
583 was tested at 29°C and 25°C. If there was no phenotype no further testing was performed. If it
584 was lethal, we tested it at 18°C.

585 Classification of Cuticle Phenotypes

586 Phenotypes were scored using a qualitative scoring system. This system used *UAS-TH RNAi* and
587 *UAS-ebony RNAi*, as a baseline for "strong". Then, lines were placed along the spectrum as mild,
588 moderate, or strong. Phenotypes were scored by two independent observers and differences
589 were settled by a third independent observer. If there was variability with one line or if there was
590 variability amongst lines, this might appear as mild-moderate, moderate-strong, or mild-strong. In
591 these cases, the strongest phenotype observed was documented as the recorded phenotype for
592 a given gene.

593 Protein-protein interaction network and gene ontology analysis

594 The protein-protein interaction network was generated using STRING (search tool for recurring
595 instances of neighboring genes, https://string-db.org/). For our data set we included these sources
596 of interactions: gene neighborhoods (genes that are found close together across species),[90]
597 curated databases (publicly available databases of protein interactions), and experimental
598 evidence (known complexes and pathways from curated sources).[92,93] Any genes that did not
599 interact with other genes from our screen were not included in the interaction network. This
600 database was last accessed on 05/05/2023. The lines between genes represents the confidence
601 in the interactions.

602 The gene ontology analysis was generated using GOrilla (Gene Ontology enRIchment anaLysis
603 and visuaLizAtion tool, https://cbl-gorilla.cs.technion.ac.il/). The 153 pigmentation genes hits were
604 included as target genes, and the background genes were the entire VDRC RNAi collection
605 included in the Mummery-Widmer et al. 2009 screen. Only the GO terms with a p-value greater
606 than 0.001 and a fold enrichment of greater than three were included in the analysis. Redundant
607 terms were removed using Revigo (http://revigo.irb.hr/) with a stringency of 0.7. Those that have
608 a fold enrichment greater than five were included in S1 Figure.

609 Human Neurological Disease Gene Classification

610 Homologs for each fly gene were identified using DIOPT (DRSC Integrative Ortholog Prediction
611 Tool, v8.0, https://www.flyrnai.org/diopt).[94] Genes were classified as orthologs if they had a
612 DIOPT score≥3. The human genes were scored as neurological disease-causing genes if they
613 had an OMIM (Online Mendelian Inheritance of Man, last accessed 01/01/2023,
614 https://www.omim.org/) disease association with any documented neurological phenotype.[95]
615 Genes were also classified as human neurological disease genes if they were in the Simons
616 Simplex Collection of Autism Spectrum Disorder gene list (last accessed 06/01/2022,
617 https://gene.sfari.org/) and had a score equal to or less than 3 (1, 2, or 3) and/or syndromic (S).[96]

618 ## Behavior Analysis using the Drosophila Activity Monitor

619 ### *Behavior screen*

620 For the behavior screen, the crosses were set in a 12:12 LD chamber at 25°C and transferred
621 every 2-3 days to increase the number of progenies. Upon eclosion, flies were transferred to 29°C
622 and kept for 2-3 more days before testing. Individual tubes (PPT5x65 Polycarbonate, Trikinetics
623 Inc, USA) appropriate for use with the *Drosophila* Activity Monitor (DAM, Model DAM2 for 5mm
624 tubes, TriKinetics Inc, USA) were loaded with approximately ½" worth of molasses-based food.
625 The end of the tube with food was sealed by placing the vial into Paraplast® (Sigma-Aldrich) wax
626 three times and allowing it to dry. Once they were dry, individual male flies were placed into each
627 vial, the vial was placed into the DAM recording chamber, and it was sealed using a 5mm tube
628 cap (CAP5, TriKinetics Inc, USA) with a hole stuffed with cotton. For each genotype, 16 individual
629 males were run, except in a few cases where we were unable to get that many flies. In which
630 case, as many living males as possible were run. The flies were loaded into a 12:12 LD chamber
631 at 29°C and monitored for 3 days. Then, the flies were removed and dead flies were eliminated
632 from analysis.

633 Locomotion and sleep analysis was run on a 24-hour period, which started at the first onset of
634 light after the flies were placed in the chamber (i.e. 18-24 hours after being placed in the chamber).
635 Locomotion was calculated based on the number of beam crossings over the full 24 hours, the
636 12 hours of light, and the 12 hours of dark. Sleep was classified as 5 minutes without any beam
637 crossings. Total Sleep was quantified as total time spent sleeping over the 12 hours of light and
638 the 12 hours of dark. Sleep latency was quantified as the amount of time after light onset or dark
639 onset before a 5-minute period of sleep. Sleep Bout Length was quantified as the average length
640 of sleep bouts (>5-minute period of sleep) during the 12 hours of light and 12 hours of dark.

641 “Outliers” were classified as lines that were more than two standard deviations from the mean of
642 all lines for any of the phenotypes scored (24-hour locomotion, 12-hour light locomotion, 12-hour
643 dark locomotion, 12-hour light total sleep, 12-hour dark total sleep, 12-hour light sleep bout length,
644 12-hour dark sleep bout length, sleep latency during the light, or sleep latency during the dark).

645 *Mask sleep study*

646 For these studies, similar tools and settings were used with these exceptions. Upon eclosion flies
647 were transferred and kept at 25°C in group housing. For the behavior without drugs, individual
648 males were placed in tubes with sucrose food (2% agar + 5% sucrose) at 3-6 dpe and behavioral
649 analysis was collected and analyzed for the following five days. Sleep was then averaged across
650 the five days for each individual fly before statistical analysis was performed. For the behavior
651 with drugs, similar conditions were followed, except data was collected on the 2-6 days after they
652 were loaded into behavior tubes to allow the drug to take effect. The following drug doses were
653 used for their respective experiments (L-DOPA: 3mg/mL L-DOPA + 12.5 µg/mL carbidopa,
654 caffeine: 0.5 mg/mL caffeine, NACA: 40 µg/mL N-acetylcysteine amide antioxidant). Drugs were
655 dissolved directly into the sucrose food except for carbidopa which was dissolve in H_2O at 1:50x
656 concentration and then added into the sucrose food.

657 High Performance Liquid Chromatography (HPLC) analysis

658 *HPLC System*

659 The HPLC used is an Antec® Scientific product with a LC110S pump, SYSTEC OEM MINI
660 Vacuum Degasser, AS110 autosampler, a SenCell flow cell with salt bridge reference electrode
661 in the Decade Lite. Data was collected and processed using DataApex Clarity™ chromatography
662 software. The column used is chosen to work well for neurotransmitters (Acquity UPLC BEH C18

663 Column, 130Å, 1.7 µm, 1 mm X 100 mm with Acquity In-Line 0.2 µm Filter). The mobile phase
664 was a 6% Acetonitrile mobile phase optimized for our samples (74.4 mg $NA_2EDTA \cdot 2H_20$, 13.72
665 mL 85% w/v phosphoric acid, 42.04 g citric acid, 1.2 g OSA, 120 mL acetonitrile, H_20 up to 2L,
666 pH=6.0 using 50% NaOH solution). The mobile phase was degassed for 10 minutes using the
667 Bransonic® Ultrasonic Bath before being loaded into the HPLC machine.

668 The standards for HPLC were made by generating master stocks of 100 mM dopamine and 10
669 mM serotonin diluted in MilliQ H_2O, which were kept at 4°C. The day of HPLC analysis, the master
670 stocks were diluted to produce standards ranging from 5-100 nM for 5-HT and 5-1000 nM for
671 dopamine. Sample concentrations of dopamine (Sigma-Aldrich, Cat#H8502) and serotonin
672 (Sigma-Aldrich, Cat#H7752) were calculated based on standards run in the same batch.
673 Standards were compared to standards run on other days to assess for overall performance.

674 *Sample Preparation*

675 For the HPLC on fly heads and brain, we adapted and modified the protocol previously
676 published.[97,98] Crosses were reared at 29°C and flies were transferred into new tubes 0-2 days
677 post eclosion (dpe). They remained at 29°C until they were 3-5 dpe. Female heads were collected
678 by anesthetizing flies with CO_2 and cutting their heads off with a razor blade. Samples were
679 collected between ZT04-ZT08. The heads were placed into 60 µL of 50 mM citrate acetate
680 (pH=4.5) and either used for analysis that day or frozen at -20°C. Five heads were used per
681 sample, and ~10 samples were run per genotype. The day of HPLC analysis, the samples were
682 thawed and grounded using a pestle for 30 seconds (Cordless Pestle Motor and Fisherbrand™
683 Disposable Pellet Pestle for 1.5mL tube). Then the samples were spun down at 13,000 rpm for
684 10 minutes. The supernatant was removed and placed into a new vial. 10 µL from each sample
685 was used for the Bradford Protein Analysis Assay. The rest of the sample solution (~40-50 µL)

686 was loaded into a vial (300 µL Polypropylene Sample Vials with 8mm Snap Caps) for HPLC
687 analysis.

688 For HPLC analysis on fly brains, flies were collected 3-7 dpe. Then, 10 fly brains (5 male, 5
689 female) were dissected in ice cold PBS. Right after dissection, the brains were transferred to 60uL
690 of ice cold 50mM citrate acetate (pH=4.5). Samples were frozen at -20°C and ran within 4 weeks
691 of collection. The day of HPLC analysis, the samples were homogenized similarly to the fly heads,
692 though for the Protein Assay, 20 µL of sample was used. Then, the remaining solution was loaded
693 for HPLC analysis.

694 *Bradford Protein Analysis Assay*

695 The Bio-Rad Bradford Assay was used for colorimetric scoring of total protein. See product details
696 for full description (Bio-Rad Protein Assay Kit I #5000001). Briefly, the dye reagent was diluted
697 1:4 in MilliQ H_2O. Then, the solution was filtered through a 0.22 µm SFCA Nalgene filter. 10 µL
698 of each protein sample (standard or fly sample) was placed into single wells of a 96-well plate.
699 Then, 200 µL of diluted 1:4 dye reagent was added to each well. The samples rested for 30-45
700 minutes and then absorbance was measured using BMG Labtech FLUOstar OPTIMA microplate
701 reader. Protein measurements for each sample were calculated based on standards ran on the
702 same plate.

703 RNA expression analysis

704 Flies were raised at 29°C until 5-7 dpe, then heads were collected by cutting them off with a razor.
705 Twenty heads were collected per sample with a mixture of males and females and placed directly
706 on dry ice. Samples were kept on dry ice or at -80°C until RNA isolation. For RNA isolation
707 samples were homogenized in 200µL of TRIzol®. Then 800µL of TRIzol® was added and the
708 samples were mixed by pipetting. The samples incubated for 5 minutes at room temperature and

709 were then spun down at 12,000 rpm for 10 minutes at 4°C. The supernatant was removed and
710 200µL of chloroform was added. The samples were mixed by shaking and then incubated at room
711 temperature for 3 minutes. Then, they were spun at 10,000 rpm for 15 minutes at 4°C, and the
712 aqueous layer was collected and placed in a new tube. 500µL of isopropanol was added and the
713 samples were left to incubate for 10 minutes at room temperature. The samples were spun at
714 10,000 rpm for 10 minutes at 4°C and the supernatant was removed. The pellet was washed with
715 1mL of 75% EtOH and centrifuged at 5,000 rpm for 5 minutes. All EtOH was removed and the
716 pellet dried at room temperature for 10 minutes. Then, the pellet was dissolved in 100µL of H_2O.
717 RNA content and quality was measured using DeNovix DS-11 Fx spectrophotometer/fluorometer.
718 cDNA reverse transcription was performed according to the iScript™ reverse transcriptase Bio-
719 Rad kit and 2 µL of RNA sample was added in a 10 µL reaction for both the reverse and no
720 reverse transcriptase reaction. Samples were measured for content and quality and then they
721 were diluted to 100ng/µL. qPCR was performed using Bio-Rad iQ SYBR Green Supermix and
722 measured on Bio-Rad CFX96™ Real-Time System. The TH primers used Forward: 5'-
723 ATGTTCGCCATCAAGAAATCCT-3' and Reverse: 5'-GGGTCTCGAAACGGGCATC-3', and the
724 control primers were for Rpl32 were Forward: 5'-ATGCTAAGCTGTCGCACAAATG-3' and
725 Reverse: 5'-GTTCGATCCGTAACCGATGT-3'. For each sample, two technical replicates were
726 run for the reverse transcriptase reaction, and the final quantity was based on the average of the
727 two. If the no reverse transcriptase reaction produced a product that was a Cq within ten, the
728 sample was discarded.

729 DAN and TH Quantification

730 Samples were stained and imaged like the brain expression analysis, except the primarily
731 antibody solution included an Elav antibody [anti-Tyrosine Hydroxylase 1:500, PelFreez
732 Biologicals, rabbit, P40101; anti-Elav 1:100, Developmental Studies Hybridoma Bank, rat,

733 7E8A10 in solution (5% Normal Donkey Serum, 0.1% NaN_3 in 0.5% PBST)]. Confocal imaging
734 was performed as described above. Once the samples were imaged, anterior, posterior, and
735 whole brain projections were generated that included all fluorescent signals from the anterior (PAL
736 and PAM clusters) and posterior (PPL1, PPM2, PPM3, PPL2ab) neuron clusters of interest. The
737 number of neurons per cluster (excluding the PAM cluster) were counted for each sample. PPM2
738 and PPM3 clusters were counted together. For TH protein quantification samples were assessed
739 using ImageJ. A boundary was drawn around each individual cluster and quantified. Then, the
740 local background for that cluster was subtracted from the cluster to give the fluorescence for the
741 given sample. Each hemisphere was treated as a separate sample.

742 Quantification and Statistical Analysis

743 Statistical analysis was performed using Graphpad Prism 10. Unless otherwise stated, all data
744 was subjected to a ROUT outlier test, where all outliers were removed, and then a one-way
745 ANOVA was performed. Each of the experimental samples were compared to the control for the
746 given samples. In the cases where there were only two samples (i.e. control and experimental),
747 a t-test was performed.

748 For the HPLC screen on heads, the samples were normalized to the controls run on that day. The
749 TRiP collection was normalized to *UAS-mCh RNAi* control and the NIG collection was normalized
750 to the *UAS-lacZ RNAi* control.

751 Supplemental Information

752 Document S1. Figures S1-S11

753 **Table S1. Screen results by RNAi line: Pigmentation, Drosophila Activity Monitor, HPLC,**
754 **and Prioritization, related to Figures 2 - 4.**

755 **Table S2. Experimental models: Organisms/strains, related to Key resources table**

References

1. Radwan, B., Liu, H., and Chaudhury, D. (2019). The role of dopamine in mood disorders and the associated changes in circadian rhythms and sleep-wake cycle. Brain Res *1713*, 42–51. https://doi.org/10.1016/J.BRAINRES.2018.11.031.
2. Grace, A.A. (2016). Dysregulation of the dopamine system in the pathophysiology of schizophrenia and depression. Nat Rev Neurosci *17*, 524–532. https://doi.org/10.1038/NRN.2016.57.
3. Nutt, D.J., Lingford-Hughes, A., Erritzoe, D., and Stokes, P.R.A. (2015). The dopamine theory of addiction: 40 years of highs and lows. Nat Rev Neurosci *16*, 305–312. https://doi.org/10.1038/NRN3939.
4. Church, F.C. (2021). Treatment Options for Motor and Non-Motor Symptoms of Parkinson's Disease. Biomolecules *11*. https://doi.org/10.3390/BIOM11040612.
5. Armstrong, M.J., and Okun, M.S. (2020). Diagnosis and Treatment of Parkinson Disease: A Review. JAMA *323*, 548–560. https://doi.org/10.1001/JAMA.2019.22360.
6. López-Cruz, L., Miguel, N.S., Carratalá-Ros, C., Monferrer, L., Salamone, J.D., and Correa, M. (2018). Dopamine depletion shifts behavior from activity based reinforcers to more sedentary ones and adenosine receptor antagonism reverses that shift: Relation to ventral striatum DARPP32 phosphorylation patterns. Neuropharmacology *138*, 349–359. https://doi.org/10.1016/J.NEUROPHARM.2018.01.034.
7. Steiner, H., and Kitai, S.T. (2001). Unilateral striatal dopamine depletion: time-dependent effects on cortical function and behavioural correlates. Eur J Neurosci *14*, 1390–1404. https://doi.org/10.1046/J.0953-816X.2001.01756.X.
8. Rohwedder, A., Wenz, N.L., Stehle, B., Huser, A., Yamagata, N., Zlatic, M., Truman, J.W., Tanimoto, H., Saumweber, T., Gerber, B., et al. (2016). Four Individually Identified

781 Paired Dopamine Neurons Signal Reward in Larval Drosophila. Curr Biol *26*, 661–669.
782 https://doi.org/10.1016/J.CUB.2016.01.012.
783 9. Budnik, V., and White, K. (1987). Genetic dissection of dopamine and serotonin synthesis
784 in the nervous system of Drosophila melanogaster. J Neurogenet *4*, 309–314.
785 https://doi.org/10.3109/01677068709167191.
786 10. Livingstone, M.S., and Tempel, B.L. (1983). Genetic dissection of monoamine
787 neurotransmitter synthesis in Drosophila. Nature *303*, 67–70.
788 https://doi.org/10.1038/303067A0.
789 11. Meiser, J., Weindl, D., and Hiller, K. (2013). Complexity of dopamine metabolism. Cell
790 Commun Signal *11*. https://doi.org/10.1186/1478-811X-11-34.
791 12. Yamamoto, S., and Seto, E.S. (2014). Dopamine dynamics and signaling in Drosophila:
792 an overview of genes, drugs and behavioral paradigms. Exp Anim *63*, 107–119.
793 https://doi.org/10.1538/EXPANIM.63.107.
794 13. Wittkopp, P.J., True, J.R., and Carroll, S.B. (2002). Reciprocal functions of the Drosophila
795 yellow and ebony proteins in the development and evolution of pigment patterns.
796 Development *129*, 1849–1858. https://doi.org/10.1242/DEV.129.8.1849.
797 14. True, J.R., Edwards, K.A., Yamamoto, D., and Carroll, S.B. (1999). Drosophila wing
798 melanin patterns form by vein-dependent elaboration of enzymatic prepatterns. Curr Biol
799 *9*, 1382–1391. https://doi.org/10.1016/S0960-9822(00)80083-4.
800 15. Spana, E.P., Abrams, A.B., Ellis, K.T., Klein, J.C., Ruderman, B.T., Shi, A.H., Zhu, D.,
801 Stewart, A., and May, S. (2020). speck, First Identified in Drosophila melanogaster in
802 1910, Is Encoded by the Arylalkalamine N-Acetyltransferase (AANAT1) Gene. G3
803 (Bethesda) *10*, 3387–3398. https://doi.org/10.1534/G3.120.401470.
804 16. Gervasi, N., Tchénio, P., and Preat, T. (2010). PKA dynamics in a Drosophila learning
805 center: coincidence detection by rutabaga adenylyl cyclase and spatial regulation by

806 dunce phosphodiesterase. Neuron *65*, 516–529.
807 https://doi.org/10.1016/J.NEURON.2010.01.014.
808 17. Heisenberg, M., Borst, A., Wagner, S., and Byers, D. (1985). Drosophila mushroom body
809 mutants are deficient in olfactory learning. J Neurogenet *2*, 1–30.
810 https://doi.org/10.3109/01677068509100140.
811 18. Jenett, A., Rubin, G.M., Ngo, T.T.B., Shepherd, D., Murphy, C., Dionne, H., Pfeiffer, B.D.,
812 Cavallaro, A., Hall, D., Jeter, J., et al. (2012). A GAL4-driver line resource for Drosophila
813 neurobiology. Cell Rep *2*, 991–1001. https://doi.org/10.1016/J.CELREP.2012.09.011.
814 19. Frighetto, G., Zordan, M.A., Castiello, U., Megighian, A., and Martin, J.R. (2022).
815 Dopamine Modulation of Drosophila Ellipsoid Body Neurons, a Nod to the Mammalian
816 Basal Ganglia. Front Physiol *13*. https://doi.org/10.3389/FPHYS.2022.849142.
817 20. Xie, T., Ho, M.C.W., Liu, Q., Horiuchi, W., Lin, C.C., Task, D., Luan, H., White, B.H.,
818 Potter, C.J., and Wu, M.N. (2018). A Genetic Toolkit for Dissecting Dopamine Circuit
819 Function in Drosophila. Cell Rep *23*, 652–665.
820 https://doi.org/10.1016/j.celrep.2018.03.068.
821 21. Clark, I.E., Dodson, M.W., Jiang, C., Cao, J.H., Huh, J.R., Seol, J.H., Yoo, S.J., Hay,
822 B.A., and Guo, M. (2006). Drosophila pink1 is required for mitochondrial function and
823 interacts genetically with parkin. Nature *441*, 1162–1166.
824 https://doi.org/10.1038/NATURE04779.
825 22. Mummery-Widmer, J.L., Yamazaki, M., Stoeger, T., Novatchkova, M., Bhalerao, S.,
826 Chen, D., Dietzl, G., Dickson, B.J., and Knoblich, J.A. (2009). Genome-wide analysis of
827 Notch signalling in Drosophila by transgenic RNAi. Nature *458*, 987–992.
828 https://doi.org/10.1038/NATURE07936.
829 23. Pendleton, R.G., Rasheed, A., Sardina, T., Tully, T., and Hillman, R. (2002). Effects of
830 Tyrosine Hydroxylase Mutants on Locomotor Activity in Drosophila: A Study in Functional
831 Genomics.

832 24. Wright, T.R.F., Bewleyz, G.C., and Sherald3, A.F. (1976). THE GENETICS OF DOPA
833 DECARBOXYLASE IN DROSOPHILA MELANOGASTER. 11. ISOLATION AND
834 CHARACTERIZATION OF DOPA-DECARBOXY LASE-DEFICIENT MUTANTS AND
835 THEIR RELATIONSHIP TO THE a-METHYL-DOPA-HYPERSENSITIVE MUTANTS.
836 25. Ni, J.Q., Liu, L.P., Binari, R., Hardy, R., Shim, H.S., Cavallaro, A., Booker, M., Pfeiffer,
837 B.D., Markstein, M., Wang, H., et al. (2009). A Drosophila resource of transgenic RNAi
838 lines for neurogenetics. Genetics *182*, 1089–1100.
839 https://doi.org/10.1534/GENETICS.109.103630.
840 26. Pan, Y., Li, W., Deng, Z., Sun, Y., Ma, X., Liang, R., Guo, X., Sun, Y., Li, W., Jiao, R., et
841 al. (2022). Myc suppresses male-male courtship in Drosophila. EMBO J *41*.
842 https://doi.org/10.15252/EMBJ.2021109905.
843 27. Riemensperger, T., Issa, A.R., Pech, U., Coulom, H., Nguyễn, M.V., Cassar, M., Jacquet,
844 M., Fiala, A., and Birman, S. (2013). A single dopamine pathway underlies progressive
845 locomotor deficits in a Drosophila model of Parkinson disease. Cell Rep *5*, 952–960.
846 https://doi.org/10.1016/J.CELREP.2013.10.032.
847 28. Brand, H., and Perrimon, N. (1993). Targeted gene expression as a means of altering cell
848 fates and generating dominant phenotypes.
849 29. Bayersdorfer, F., Voigt, A., Schneuwly, S., and Botella, J.A. (2010). Dopamine-dependent
850 neurodegeneration in Drosophila models of familial and sporadic Parkinson's disease.
851 Neurobiol Dis *40*, 113–119. https://doi.org/10.1016/J.NBD.2010.02.012.
852 30. Hovemann, B.T., Ryseck, R.P., Walldorf, U., Störtkuhl, K.F., Dietzel, I.D., and Dessen, E.
853 (1998). The Drosophila ebony gene is closely related to microbial peptide synthetases
854 and shows specific cuticle and nervous system expression. Gene *221*, 1–9.
855 https://doi.org/10.1016/S0378-1119(98)00440-5.

856 31. Richardt, A., Rybak, J., Störtkuhl, K.F., Meinertzhagen, I.A., and Hovemann, B.T. (2002).
857 Ebony protein in the Drosophila nervous system: optic neuropile expression in glial cells.
858 J Comp Neurol *452*, 93–102. https://doi.org/10.1002/CNE.10360.
859 32. Yamamoto-Hino, M., Yoshida, H., Ichimiya, T., Sakamura, S., Maeda, M., Kimura, Y.,
860 Sasaki, N., Aoki-Kinoshita, K.F., Kinoshita-Toyoda, A., Toyoda, H., et al. (2015).
861 Phenotype-based clustering of glycosylation-related genes by RNAi-mediated gene
862 silencing. Genes to Cells *20*, 521–542. https://doi.org/10.1111/gtc.12246.
863 33. Riemensperger, T., Isabel, G., Coulom, H., Neuser, K., Seugnet, L., Kume, K., Iché-
864 Torres, M., Cassar, M., Strauss, R., Preat, T., et al. (2011). Behavioral consequences of
865 dopamine deficiency in the Drosophila central nervous system. Proc Natl Acad Sci U S A
866 *108*, 834–839. https://doi.org/10.1073/pnas.1010930108.
867 34. Chiu, J.C., Low, K.H., Pike, D.H., Yildirim, E., and Edery, I. (2010). Assaying locomotor
868 activity to study circadian rhythms and sleep parameters in Drosophila. Journal of
869 Visualized Experiments. https://doi.org/10.3791/2157.
870 35. Dietzl, G., Chen, D., Schnorrer, F., Su, K.C., Barinova, Y., Fellner, M., Gasser, B.,
871 Kinsey, K., Oppel, S., Scheiblauer, S., et al. (2007). A genome-wide transgenic RNAi
872 library for conditional gene inactivation in Drosophila. Nature *448*, 151–156.
873 https://doi.org/10.1038/NATURE05954.
874 36. Ni, J.Q., Zhou, R., Czech, B., Liu, L.P., Holderbaum, L., Yang-Zhou, D., Shim, H.S., Tao,
875 R., Handler, D., Karpowicz, P., et al. (2011). A genome-scale shRNA resource for
876 transgenic RNAi in Drosophila. Nat Methods *8*, 405–407.
877 https://doi.org/10.1038/NMETH.1592.
878 37. Vissers, J.H.A., Manning, S.A., Kulkarni, A., and Harvey, K.F. (2016). A Drosophila RNAi
879 library modulates Hippo pathway-dependent tissue growth. Nature Communications 2016
880 7:1 *7*, 1–6. https://doi.org/10.1038/ncomms10368.

881 38. Shafer, O.T., and Keene, A.C. (2021). The Regulation of Drosophila Sleep. Preprint at
882 Cell Press, https://doi.org/10.1016/j.cub.2020.10.082
883 https://doi.org/10.1016/j.cub.2020.10.082.
884 39. Diao, F., Ironfield, H., Luan, H., Diao, F., Shropshire, W.C., Ewer, J., Marr, E., Potter,
885 C.J., Landgraf, M., and White, B.H. (2015). Plug-and-play genetic access to drosophila
886 cell types using exchangeable exon cassettes. Cell Rep *10*, 1410–1421.
887 https://doi.org/10.1016/J.CELREP.2015.01.059.
888 40. Lee, P.T., Zirin, J., Kanca, O., Lin, W.W., Schulze, K.L., Li-Kroeger, D., Tao, R.,
889 Devereaux, C., Hu, Y., Chung, V., et al. (2018). A gene-specific T2A-GAL4 library for
890 Drosophila. Elife *7*. https://doi.org/10.7554/ELIFE.35574.
891 41. Kanca, O., Zirin, J., Garcia-Marques, J., Knight, S.M., Yang-Zhou, D., Amador, G.,
892 Chung, H., Zuo, Z., Ma, L., He, Y., et al. (2019). An efficient CRISPR-based strategy to
893 insert small and large fragments of DNA using short homology arms. Elife *8*, e51539.
894 https://doi.org/10.7554/eLife.51539.
895 42. Janssens, J., Aibar, S., Taskiran, I.I., Ismail, J.N., Gomez, A.E., Aughey, G., Spanier, K.I.,
896 Rop, F.V. De, González-Blas, C.B., Dionne, M., et al. (2022). Decoding gene regulation in
897 the fly brain. Nature *601*, 630–636. https://doi.org/10.1038/S41586-021-04262-Z.
898 43. Li, H., Janssens, J., de Waegeneer, M., Kolluru, S.S., Davie, K., Gardeux, V., Saelens,
899 W., David, F.P.A., Brbić, M., Spanier, K., et al. (2022). Fly Cell Atlas: A single-nucleus
900 transcriptomic atlas of the adult fruit fly. Science (1979) *375*.
901 https://doi.org/10.1126/science.abk2432.
902 44. Morin, X., Daneman, R., Zavortink, M., and Chia, W. A protein trap strategy to detect
903 GFP-tagged proteins expressed from their endogenous loci in Drosophila.
904 45. Buszczak, M., Paterno, S., Lighthouse, D., Bachman, J., Planck, J., Owen, S., Skora,
905 A.D., Nystul, T.G., Ohlstein, B., Allen, A., et al. (2007). The carnegie protein trap library: A

906 versatile tool for drosophila developmental studies. Genetics *175*, 1505–1531.
907 https://doi.org/10.1534/genetics.106.065961.
908 46. Mao, Z., and Davis, R.L. (2009). Eight different types of dopaminergic neurons innervate
909 the Drosophila mushroom body neuropil: Anatomical and physiological heterogeneity.
910 Front Neural Circuits *3*, 5. https://doi.org/10.3389/NEURO.04.005.2009/BIBTEX.
911 47. Voet, M. Van Der, Harich, B., Franke, B., and Schenck, A. (2016). ADHD-associated
912 dopamine transporter, latrophilin and neurofibromin share a dopamine-related locomotor
913 signature in Drosophila. Mol Psychiatry *21*, 565–573. https://doi.org/10.1038/mp.2015.55.
914 48. Kume, K., Kume, S., Park, S.K., Hirsh, J., and Jackson, F.R. (2005). Dopamine is a
915 regulator of arousal in the fruit fly. Journal of Neuroscience *25*, 7377–7384.
916 https://doi.org/10.1523/JNEUROSCI.2048-05.2005.
917 49. Nall, A.H., Shakhmantsir, I., Cichewicz, K., Birman, S., Hirsh, J., and Sehgal, A. (2016).
918 Caffeine promotes wakefulness via dopamine signaling in Drosophila. Sci Rep *6*.
919 https://doi.org/10.1038/srep20938.
920 50. Ni, J.Q., Markstein, M., Binari, R., Pfeiffer, B., Liu, L.P., Villalta, C., Booker, M., Perkins,
921 L., and Perrimon, N. (2007). Vector and parameters for targeted transgenic RNA
922 interference in Drosophila melanogaster. Nature Methods 2008 5:1 *5*, 49–51.
923 https://doi.org/10.1038/nmeth1146.
924 51. McGary, K.L., Park, T.J., Woods, J.O., Cha, H.J., Wallingford, J.B., and Marcotte, E.M.
925 (2010). Systematic discovery of nonobvious human disease models through orthologous
926 phenotypes. Proc Natl Acad Sci U S A *107*, 6544–6549.
927 https://doi.org/10.1073/pnas.0910200107.
928 52. Nakashima, A., Ohnuma, S., Kodani, Y., Kaneko, Y.S., Nagasaki, H., Nagatsu, T., and
929 Ota, A. (2016). Inhibition of deubiquitinating activity of USP14 decreases tyrosine
930 hydroxylase phosphorylated at Ser19 in PC12D cells. Biochem Biophys Res Commun
931 *472*, 598–602. https://doi.org/10.1016/J.BBRC.2016.03.022.

932 53. Kawahata, I., Ohtaku, S., Tomioka, Y., Ichinose, H., and Yamakuni, T. (2015). Dopamine
933 or biopterin deficiency potentiates phosphorylation at (40)Ser and ubiquitination of
934 tyrosine hydroxylase to be degraded by the ubiquitin proteasome system. Biochem
935 Biophys Res Commun *465*, 53–58. https://doi.org/10.1016/J.BBRC.2015.07.125.
936 54. Birman, S., Morgan, B., Anzivino, M., and Hirsh, J. (1994). A novel and major isoform of
937 tyrosine hydroxylase in Drosophila is generated by alternative RNA processing. Journal
938 of Biological Chemistry *269*, 26559–26567. https://doi.org/10.1016/S0021-
939 9258(18)47231-6.
940 55. Vié, A., Cigna, M., Toci, R., and Birman, S. (1999). Differential regulation of Drosophila
941 tyrosine hydroxylase isoforms by dopamine binding and cAMP-dependent
942 phosphorylation. J Biol Chem *274*, 16788–16795.
943 https://doi.org/10.1074/JBC.274.24.16788.
944 56. Gervasi, N.M., Scott, S.S., Aschrafi, A., Gale, J., Vohra, S.N., Macgibeny, M.A., Kar,
945 A.N., Gioio, A.E., and Kaplan, B.B. (2016). The local expression and trafficking of tyrosine
946 hydroxylase mRNA in the axons of sympathetic neurons. RNA *22*, 883–895.
947 https://doi.org/10.1261/RNA.053272.115.
948 57. Freeman, A., Pranski, E., Miller, R.D., Radmard, S., Bernhard, D., Jinnah, H.A., Betarbet,
949 R., Rye, D.B., and Sanyal, S. (2012). Sleep fragmentation and motor restlessness in a
950 Drosophila model of Restless Legs Syndrome. Current Biology *22*, 1142.
951 https://doi.org/10.1016/J.CUB.2012.04.027.
952 58. Chaudhuri, A., Bowling, K., Funderburk, C., Lawal, H., Inamdar, A., Wang, Z., and
953 O'Donnell, J.M. (2007). Interaction of Genetic and Environmental Factors in a Drosophila
954 Parkinsonism Model. The Journal of Neuroscience *27*, 2457.
955 https://doi.org/10.1523/JNEUROSCI.4239-06.2007.
956 59. Wang, Z., Ferdousy, F., Lawal, H., Huang, Z., Daigle, J.G., Izevbaye, I., Doherty, O.,
957 Thomas, J., Stathakis, D.G., and O'Donnell, J.M. (2011). Catecholamines up integrates

958 dopamine synthesis and synaptic trafficking. J Neurochem *119*, 1294–1305.
959 https://doi.org/10.1111/J.1471-4159.2011.07517.X.
960 60. Zhang, Y.Q., Friedman, D.B., Wang, Z., Woodruff, E., Pan, L., O'Donnell, J., and Broadie,
961 K. (2005). Protein expression profiling of the Drosophila fragile X mutant brain reveals up-
962 regulation of monoamine synthesis. Molecular and Cellular Proteomics *4*, 278–290.
963 https://doi.org/10.1074/mcp.M400174-MCP200.
964 61. Wicker-Thomas, C., and Hamann, M. (2008). Interaction of dopamine, female
965 pheromones, locomotion and sex behavior in Drosophila melanogaster. J Insect Physiol
966 *54*, 1423–1431. https://doi.org/10.1016/j.jinsphys.2008.08.005.
967 62. Takahashi, A. (2013). Pigmentation and behavior: potential association through
968 pleiotropic genes in Drosophila.
969 63. Letizia, A., Bario, R., and Campuzano, S. (2007). Antagonistic and cooperative actions of
970 the EGFR and Dpp pathways on the iroquois genes regulate Drosophila mesothorax
971 specification and patterning. Development *134*, 1337–1346.
972 https://doi.org/10.1242/DEV.02823.
973 64. Lu, J., Wang, Y., Wang, X., Wang, D., Pflugfelder, G.O., and Shen, J. (2022). The Tbx6
974 Transcription Factor Dorsocross Mediates Dpp Signaling to Regulate Drosophila Thorax
975 Closure. Int J Mol Sci *23*. https://doi.org/10.3390/IJMS23094543.
976 65. Zeitlinger, J., and Bohmann, D. (1999). Thorax closure in Drosophila: involvement of Fos
977 and the JNK pathway. Development *126*, 3947–3956.
978 https://doi.org/10.1242/DEV.126.17.3947.
979 66. Massey, J.H., Akiyama, N., Bien, T., Dreisewerd, K., Wittkopp, P.J., Yew, J.Y., and
980 Takahashi, A. (2019). Pleiotropic Effects of ebony and tan on Pigmentation and Cuticular
981 Hydrocarbon Composition in Drosophila melanogaster. Front Physiol *10*, 518.
982 https://doi.org/10.3389/FPHYS.2019.00518/BIBTEX.

983 67. Zhang, S., Wang, R., and Wang, G. (2019). Impact of Dopamine Oxidation on
984 Dopaminergic Neurodegeneration. ACS Chem Neurosci *10*, 945–953.
985 https://doi.org/10.1021/ACSCHEMNEURO.8B00454/ASSET/IMAGES/MEDIUM/CN-
986 2018-004545_0005.GIF.
987 68. Davla, S., Artiushin, G., Li, Y., Chitsaz, D., Li, S., Sehgal, A., and van Meyel, D.J. (2020).
988 AANAT1 functions in astrocytes to regulate sleep homeostasis. Elife *9*, 1–48.
989 https://doi.org/10.7554/ELIFE.53994.
990 69. DeAngelis, M.W., McGhie, E.W., Coolon, J.D., and Johnson, R.I. (2020). Mask, a
991 component of the Hippo pathway, is required for Drosophila eye morphogenesis. Dev Biol
992 *464*, 53–70. https://doi.org/10.1016/j.ydbio.2020.05.002.
993 70. Zhu, M., Zhang, S., Tian, X., and Wu, C. (2017). Mask mitigates MAPT- and FUS-
994 induced degeneration by enhancing autophagy through lysosomal acidification.
995 Autophagy *13*, 1924–1938. https://doi.org/10.1080/15548627.2017.1362524.
996 71. Martinez, D., Zhu, M., Guidry, J.J., Majeste, N., Mao, H., Yanofsky, S.T., Tian, X., and
997 Wu, C. (2021). Mask, the Drosophila ankyrin repeat and KH domain-containing protein,
998 affects microtubule stability. J Cell Sci *134*. https://doi.org/10.1242/jcs.258512.
999 72. Dubowy, C., and Sehgal, A. (2017). Circadian rhythms and sleep in Drosophila
1000 melanogaster. Genetics *205*, 1373–1397. https://doi.org/10.1534/genetics.115.185157.
1001 73. Cichewicz, K., Garren, E.J., Adiele, C., Aso, Y., Wang, Z., Wu, M., Birman, S., Rubin,
1002 G.M., and Hirsh, J. (2017). A new brain dopamine-deficient Drosophila and its
1003 pharmacological and genetic rescue. Genes Brain Behav *16*, 394–403.
1004 https://doi.org/10.1111/GBB.12353.
1005 74. Sidor, C.M., Brain, R., and Thompson, B.J. (2013). Mask proteins are cofactors of
1006 Yorkie/YAP in the Hippo pathway. Curr Biol *23*, 223–228.
1007 https://doi.org/10.1016/J.CUB.2012.11.061.

1008 75. Sansores-Garcia, L., Atkins, M., Moya, I.M., Shahmoradgoli, M., Tao, C., Mills, G.B., and
1009 Halder, G. (2013). Mask is required for the activity of the Hippo pathway effector Yki/YAP.
1010 Curr Biol *23*, 229–235. https://doi.org/10.1016/J.CUB.2012.12.033.
1011 76. Smith, R.K., Carroll, P.M., Allard, J.D., and Simon, M.A. (2002). MASK, a large ankyrin
1012 repeat and KH domain-containing protein involved in Drosophila receptor tyrosine kinase
1013 signaling. Development *129*, 71–82. https://doi.org/10.1242/DEV.129.1.71.
1014 77. Zhu, M., Li, X., Tian, X., and Wu, C. (2015). Mask loss-of-function rescues mitochondrial
1015 impairment and muscle degeneration of Drosophila pink1 and parkin mutants. Hum Mol
1016 Genet *24*, 3272–3285. https://doi.org/10.1093/HMG/DDV081.
1017 78. Lusk, J.B., Lam, V.Y.M., and Tolwinski, N.S. (2017). Epidermal Growth Factor Pathway
1018 Signaling in Drosophila Embryogenesis: Tools for Understanding Cancer. Cancers
1019 (Basel) *9*. https://doi.org/10.3390/CANCERS9020016.
1020 79. Oh, H., and Irvine, K.D. (2010). Yorkie: the final destination of Hippo signaling. Trends
1021 Cell Biol *20*, 410. https://doi.org/10.1016/J.TCB.2010.04.005.
1022 80. Sen, A., Kalvakuri, S., Bodmer, R., and Cox, R.T. (2015). Clueless, a protein required for
1023 mitochondrial function, interacts with the PINK1-Parkin complex in Drosophila. Dis Model
1024 Mech *8*, 577–589. https://doi.org/10.1242/DMM.019208.
1025 81. Wang, Z.H., Clark, C., and Geisbrecht, E.R. (2016). Drosophila clueless is involved in
1026 Parkin-dependent mitophagy by promoting VCP-mediated Marf degradation. Hum Mol
1027 Genet *25*, 1946–1964. https://doi.org/10.1093/HMG/DDW067.
1028 82. Sen, A., and Cox, R.T. (2016). Clueless is a conserved ribonucleoprotein that binds the
1029 ribosome at the mitochondrial outer membrane. Biol Open *5*, 195–203.
1030 https://doi.org/10.1242/BIO.015313/-/DC1.
1031 83. Inagaki, H.K., De-Leon, S.B.-T., Wong, A.M., Jagadish, S., Ishimoto, H., Barnea, G.,
1032 Kitamoto, T., Axel, R., and Anderson, D.J. (2012). Visualizing Neuromodulation In Vivo:

1033 TANGO-Mapping of Dopamine Signaling Reveals Appeptite Control of Sugar Sensing.
1034 Cell *148*, 583. https://doi.org/10.1016/J.CELL.2011.12.022.
1035 84. Sun, F., Zhou, J., Dai, B., Qian, T., Zeng, J., Li, X., Zhuo, Y., Zhang, Y., Wang, Y., Qian,
1036 C., et al. (2020). Next-generation GRAB sensors for monitoring dopaminergic activity in
1037 vivo. Nat Methods *17*, 1156. https://doi.org/10.1038/S41592-020-00981-9.
1038 85. Kasture, A.S., Hummel, T., Sucic, S., and Freissmuth, M. (2018). Big Lessons from Tiny
1039 Flies: Drosophila melanogaster as a Model to Explore Dysfunction of Dopaminergic and
1040 Serotonergic Neurotransmitter Systems. Int J Mol Sci *19*.
1041 https://doi.org/10.3390/IJMS19061788.
1042 86. Calleja, M., Herranz, H., Estella, C., Casal, J., Lawrence, P., Simpson, P., and Morata, G.
1043 (2000). Generation of medial and lateral dorsal body domains by the pannier gene of
1044 Drosophila. Development *127*, 3971–3980. https://doi.org/10.1242/DEV.127.18.3971.
1045 87. Kennerdell, J.R., and Carthew, R.W. (2000). Heritable gene silencing in Drosophila using
1046 double-stranded RNA. Nat Biotechnol *18*, 896–898. https://doi.org/10.1038/78531.
1047 88. Yamamoto, S., Charng, W.L., Rana, N.A., Kakuda, S., Jaiswal, M., Bayat, V., Xiong, B.,
1048 Zhang, K., Sandoval, H., David, G., et al. (2012). A mutation in EGF repeat-8 of notch
1049 discriminates between serrate/jagged and delta family ligands. Science (1979) *338*,
1050 1229–1232. https://doi.org/10.1126/science.1228745.
1051 89. Marcogliese, P.C., Deal, S.L., Andrews, J., Harnish, J.M., Bhavana, V.H., Graves, H.K.,
1052 Jangam, S., Luo, X., Liu, N., Bei, D., et al. (2022). Drosophila functional screening of de
1053 novo variants in autism uncovers damaging variants and facilitates discovery of rare
1054 neurodevelopmental diseases. Cell Rep *38*. https://doi.org/10.1016/j.celrep.2022.110517.
1055 90. Snel, B., Lehmann, G., Bork, P., and Huynen, M.A. (2000). STRING: a web-server to
1056 retrieve and display the repeatedly occurring neighbourhood of a gene.
1057 91. Davie, K., Janssens, J., Koldere, D., De Waegeneer, M., Pech, U., Kreft, Ł., Aibar, S.,
1058 Makhzami, S., Christiaens, V., Bravo González-Blas, C., et al. (2018). A Single-Cell

1059 Transcriptome Atlas of the Aging Drosophila Brain. Cell *174*, 982-998.e20.
1060 https://doi.org/10.1016/j.cell.2018.05.057.
1061 92. Szklarczyk, D., Gable, A.L., Nastou, K.C., Lyon, D., Kirsch, R., Pyysalo, S., Doncheva,
1062 N.T., Legeay, M., Fang, T., Bork, P., et al. (2021). The STRING database in 2021:
1063 Customizable protein-protein networks, and functional characterization of user-uploaded
1064 gene/measurement sets. Nucleic Acids Res *49*, D605–D612.
1065 https://doi.org/10.1093/nar/gkaa1074.
1066 93. Szklarczyk, D., Kirsch, R., Koutrouli, M., Nastou, K., Mehryary, F., Hachilif, R., Gable,
1067 A.L., Fang, T., Doncheva, N.T., Pyysalo, S., et al. (2023). The STRING database in 2023:
1068 protein-protein association networks and functional enrichment analyses for any
1069 sequenced genome of interest. Nucleic Acids Res *51*, D638–D646.
1070 https://doi.org/10.1093/nar/gkac1000.
1071 94. Hu, Y., Flockhart, I., Vinayagam, A., Bergwitz, C., Berger, B., Perrimon, N., and Mohr,
1072 S.E. (2011). An integrative approach to ortholog prediction for disease-focused and other
1073 functional studies. BMC Bioinformatics *12*. https://doi.org/10.1186/1471-2105-12-357.
1074 95. Hamosh, A., Amberger, J.S., Bocchini, C., Scott, A.F., and Rasmussen, S.A. (2021).
1075 Online Mendelian Inheritance in Man (OMIM®): Victor McKusick's magnum opus. Am J
1076 Med Genet A *185*, 3259–3265. https://doi.org/10.1002/ajmg.a.62407.
1077 96. Abrahams, B.S., Arking, D.E., Campbell, D.B., Mefford, H.C., Morrow, E.M., Weiss, L.A.,
1078 Menashe, I., Wadkins, T., Banerjee-Basu, S., and Packer, A. (2013). SFARI Gene 2.0: A
1079 community-driven knowledgebase for the autism spectrum disorders (ASDs). Mol Autism
1080 *4*. https://doi.org/10.1186/2040-2392-4-36.
1081 97. Cichewicz, K., Garren, E.J., Adiele, C., Aso, Y., Wang, Z., Wu, M., Birman, S., Rubin,
1082 G.M., and Hirsh, J. (2017). A new brain dopamine-deficient Drosophila and its
1083 pharmacological and genetic rescue. Genes Brain Behav *16*, 394–403.
1084 https://doi.org/10.1111/gbb.12353.

1085 98. Hardie, S.L., and Hirsh, J. (2006). An improved method for the separation and detection
1086 of biogenic amines in adult Drosophila brain extracts by high performance liquid
1087 chromatography. J Neurosci Methods *153*, 243–249.
1088 https://doi.org/10.1016/j.jneumeth.2005.11.001.
1089
1090

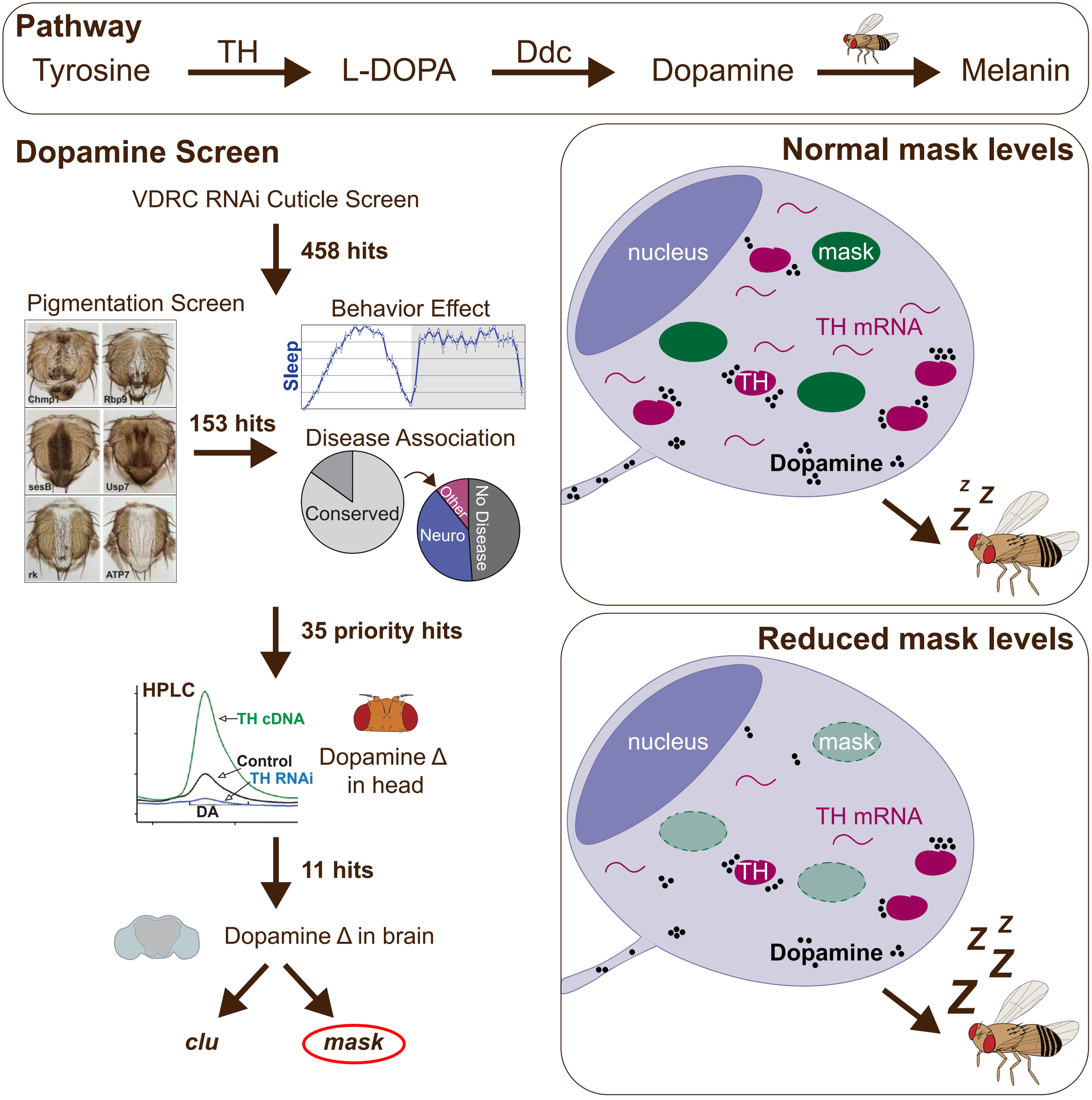
Pathway
Tyrosine
TH
L-DOPA
Ddc
Dopamine
Melanin
Dopamine Screen
VDRC RNAi Cuticle Screen
458 hits
Pigmentation Screen
Chmp1
Rbp9
sesB
Usp7
rk
ATP7
153 hits
Behavior Effect
Sleep
Disease Association
Conserved
Other
Neuro
No Disease
35 priority hits
HPLC
TH cDNA
Control
TH RNAi
DA
Dopamine Δ
in head
11 hits
Dopamine Δ in brain
clu
mask
Normal mask levels
nucleus
mask
TH mRNA
TH
Dopamine
Reduced mask levels
nucleus
mask
TH mRNA
TH
Dopamine

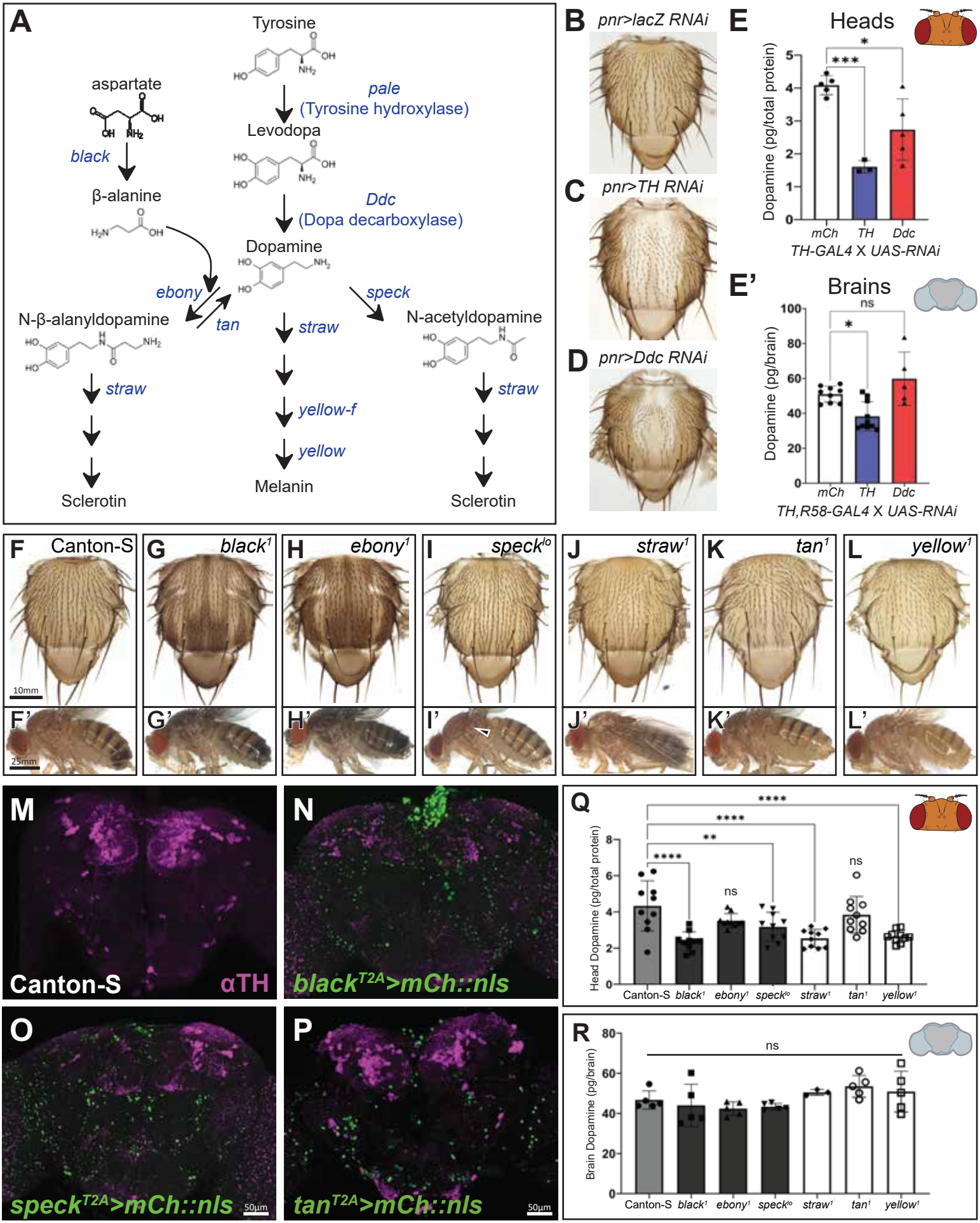
A
Tyrosine
aspartate
pale
(Tyrosine hydroxylase)
Levodopa
black
β-alanine
Ddc
(Dopa decarboxylase)
Dopamine
ebony
tan
speck
N-β-alanyldopamine
N-acetyldopamine
straw
straw
straw
yellow-f
yellow
Sclerotin
Melanin
Sclerotin
B pnr>lacZ RNAi
C pnr>TH RNAi
D pnr>Ddc RNAi
E Heads
Dopamine (pg/total protein)
mCh TH Ddc
TH-GAL4 X UAS-RNAi
E' Brains
Dopamine (pg/brain)
mCh TH Ddc
TH,R58-GAL4 X UAS-RNAi
F Canton-S
G black1
H ebony1
I specklo
J straw1
K tan1
L yellow1
10mm
25mm
M
Canton-S αTH
N
black T2A>mCh::nls
O
speck T2A>mCh::nls
50µm
P
tan T2A>mCh::nls
50µm
Q
Head Dopamine (pg/total protein)
Canton-S black1 ebony1 specklo straw1 tan1 yellow1
R
Brain Dopamine (pg/brain)
Canton-S black1 ebony1 specklo straw1 tan1 yellow1

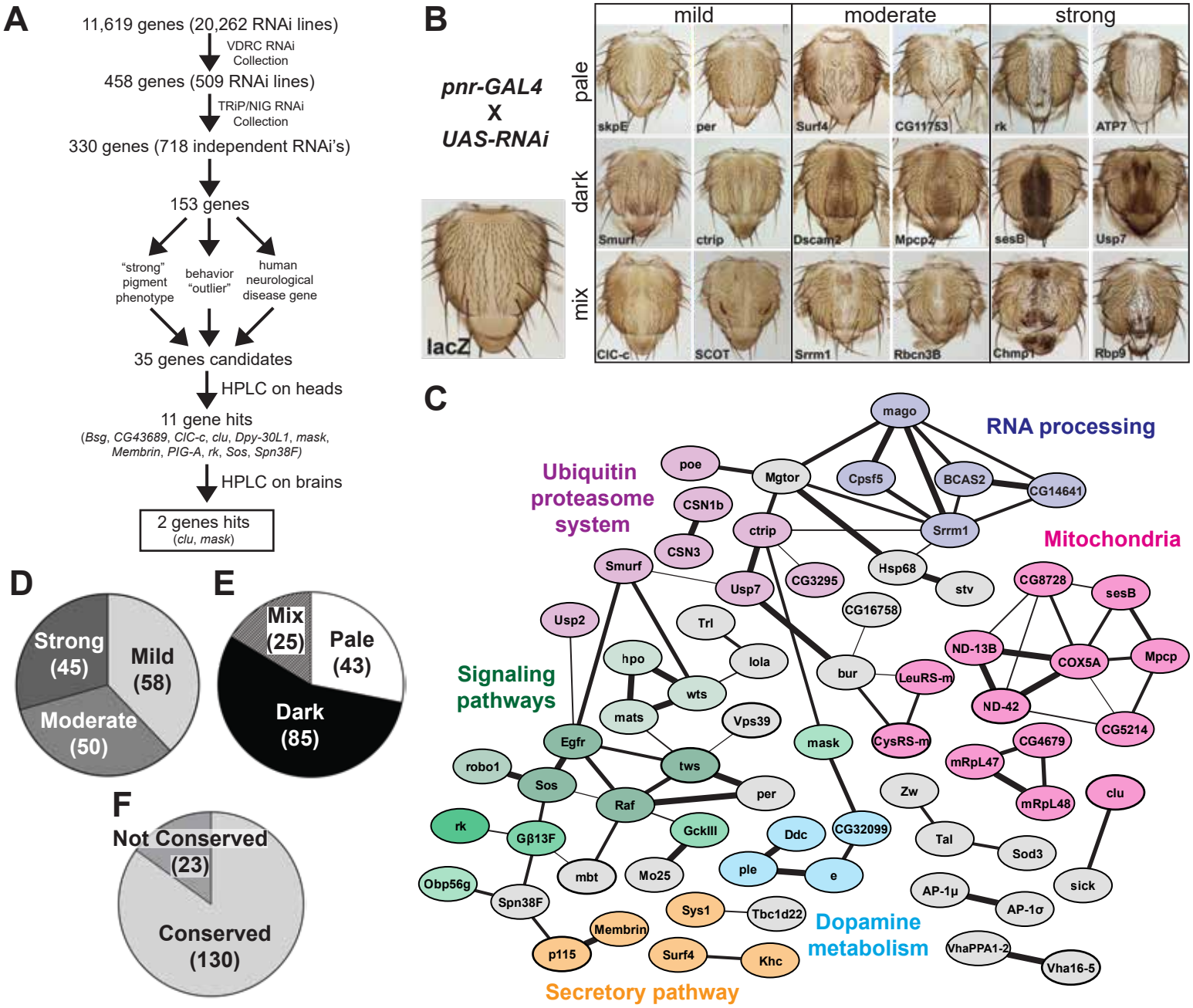
A
11,619 genes (20,262 RNAi lines)
VDRC RNAi Collection
458 genes (509 RNAi lines)
TRiP/NIG RNAi Collection
330 genes (718 independent RNAi's)
153 genes
"strong" pigment phenotype
behavior "outlier"
human neurological disease gene
35 genes candidates
HPLC on heads
11 gene hits
(Bsg, CG43689, ClC-c, clu, Dpy-30L1, mask, Membrin, PIG-A, rk, Sos, Spn38F)
HPLC on brains
2 genes hits
(clu, mask)
B
pnr-GAL4
x
UAS-RNAi
lacZ
mild
moderate
strong
pale
dark
mix
skpE
per
Surf4
CG11753
rk
ATP7
Smurf
ctrip
Dscam2
Mpcp2
sesB
Usp7
ClC-c
SCOT
Srrm1
Rbcn3B
Chmp1
Rbp9
C
RNA processing
Ubiquitin proteasome system
Mitochondria
Signaling pathways
Dopamine metabolism
Secretory pathway
mago
poe
Mgtor
Cpsf5
BCAS2
CG14641
CSN1b
ctrip
Srrm1
CSN3
Smurf
Hsp68
Usp7
CG3295
stv
CG8728
sesB
CG16758
Usp2
Trl
ND-13B
COX5A
Mpcp
hpo
lola
bur
LeuRS-m
wts
ND-42
mats
Vps39
CG5214
Egfr
mask
CysRS-m
CG4679
robo1
tws
mRpL47
Sos
per
Zw
clu
Raf
mRpL48
rk
Gβ13F
GckIII
Ddc
CG32099
Tal
Sod3
mbt
Mo25
ple
e
Obp56g
sick
Spn38F
AP-1μ
AP-1σ
Sys1
Tbc1d22
Membrin
VhaPPA1-2
p115
Surf4
Khc
Vha16-5
D
Strong (45)
Mild (58)
Moderate (50)
E
Mix (25)
Pale (43)
Dark (85)
F
Not Conserved (23)
Conserved (130)

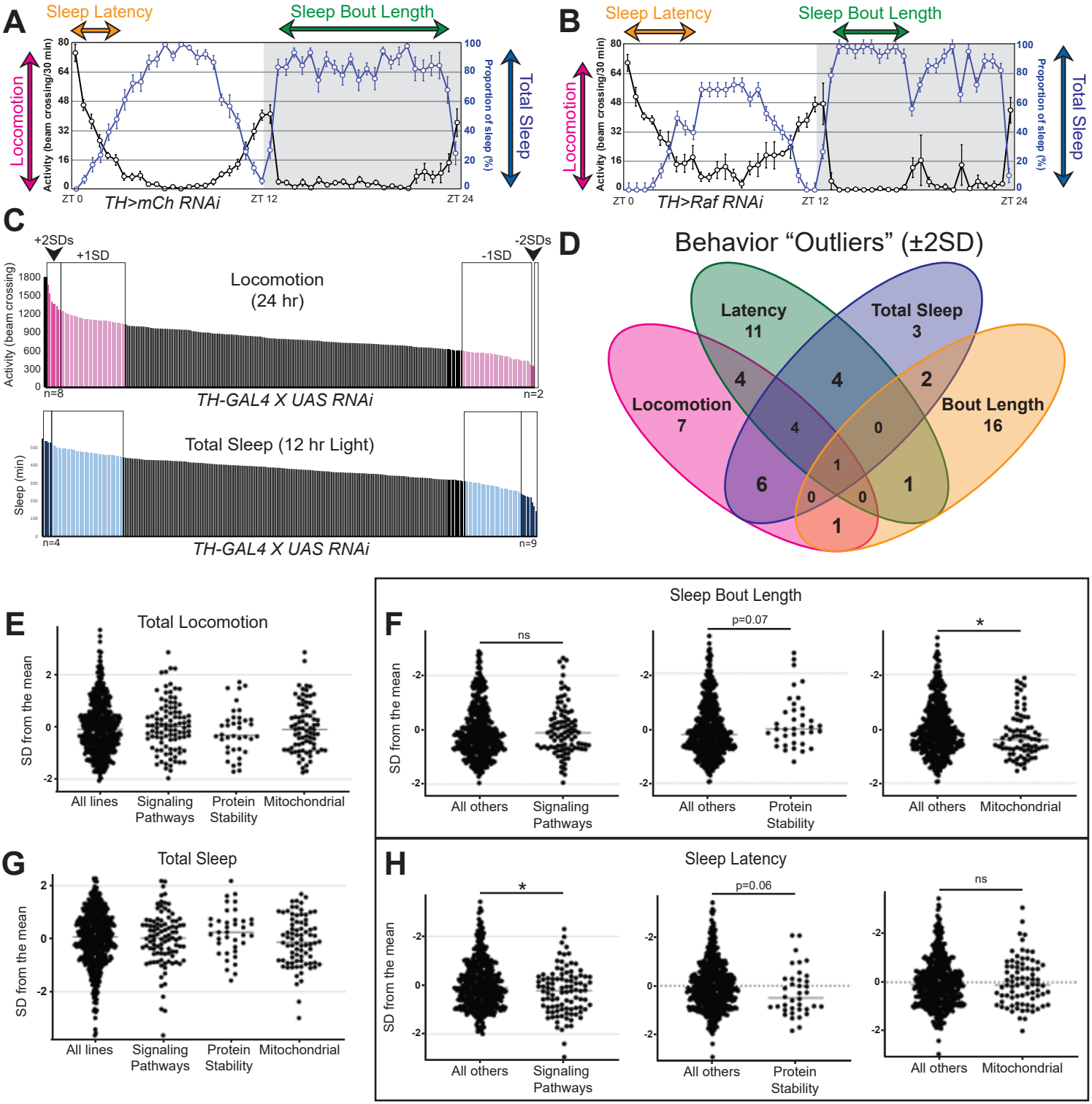
A
Sleep Latency
Sleep Bout Length
Locomotion
Total Sleep
Activity (beam crossing/30 min)
Proportion of sleep (%)
ZT 0
ZT 12
ZT 24
TH>mCh RNAi
B
TH>Raf RNAi
C
+2SDs
+1SD
-1SD
-2SDs
Locomotion
(24 hr)
Activity (beam crossing)
n=8
n=2
TH-GAL4 X UAS RNAi
Total Sleep (12 hr Light)
Sleep (min)
n=4
n=9
D
Behavior "Outliers" (±2SD)
Latency
11
Total Sleep
3
Locomotion
7
Bout Length
16
E
Total Locomotion
SD from the mean
All lines
Signaling Pathways
Protein Stability
Mitochondrial
F
Sleep Bout Length
ns
p=0.07
*
All others
G
Total Sleep
H
Sleep Latency
p=0.06

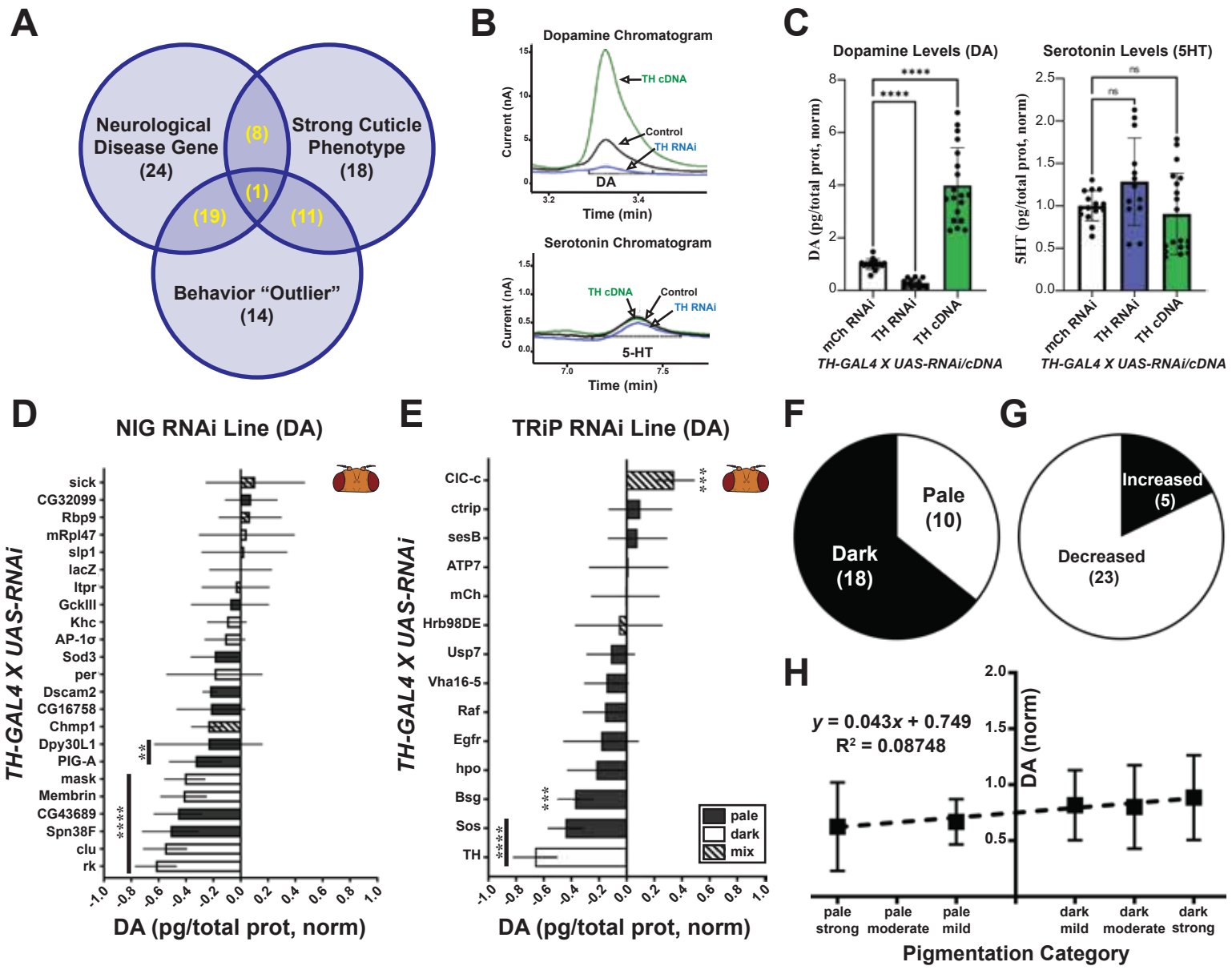
A
Neurological Disease Gene (24)
Strong Cuticle Phenotype (18)
Behavior "Outlier" (14)
(8)
(1)
(19)
(11)
B
Dopamine Chromatogram
TH cDNA
Control
TH RNAi
DA
Current (nA)
Time (min)
Serotonin Chromatogram
TH cDNA
Control
TH RNAi
5-HT
Current (nA)
Time (min)
C
Dopamine Levels (DA)
Serotonin Levels (5HT)
DA (pg/total prot, norm)
5HT (pg/total prot, norm)
mCh RNAi
TH RNAi
TH cDNA
TH-GAL4 X UAS-RNAi/cDNA
D
NIG RNAi Line (DA)
TH-GAL4 X UAS-RNAi
sick
CG32099
Rbp9
mRpl47
slp1
lacZ
Itpr
GckIII
Khc
AP-1σ
Sod3
per
Dscam2
CG16758
Chmp1
Dpy30L1
PIG-A
mask
Membrin
CG43689
Spn38F
clu
rk
DA (pg/total prot, norm)
E
TRiP RNAi Line (DA)
TH-GAL4 X UAS-RNAi
CIC-c
ctrip
sesB
ATP7
mCh
Hrb98DE
Usp7
Vha16-5
Raf
Egfr
hpo
Bsg
Sos
TH
pale
dark
mix
DA (pg/total prot, norm)
F
Pale (10)
Dark (18)
G
Increased (5)
Decreased (23)
H
y = 0.043x + 0.749
R² = 0.08748
DA (norm)
pale strong
pale moderate
pale mild
dark mild
dark moderate
dark strong
Pigmentation Category

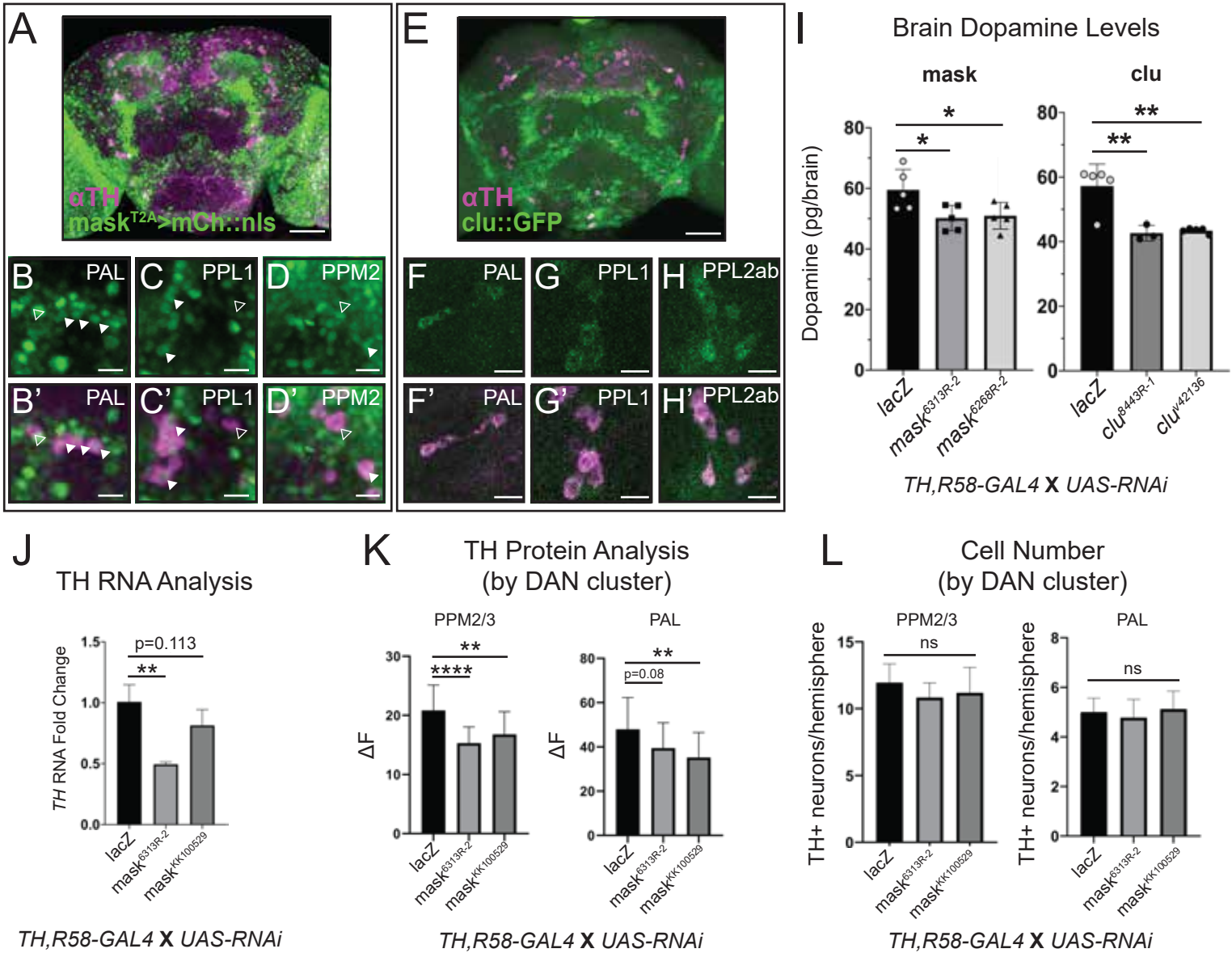
A
αTH
mask^T2A>mCh::nls
B PAL
C PPL1
D PPM2
B' PAL
C' PPL1
D' PPM2
E
αTH
clu::GFP
F PAL
G PPL1
H PPL2ab
F' PAL
G' PPL1
H' PPL2ab
I
Brain Dopamine Levels
mask
clu
Dopamine (pg/brain)
lacZ
mask^6313R-2
mask^6268R-2
clu^8443R-1
clu^v42136
TH,R58-GAL4 X UAS-RNAi
J
TH RNA Analysis
TH RNA Fold Change
p=0.113
lacZ
mask^6313R-2
mask^KK100529
TH,R58-GAL4 X UAS-RNAi
K
TH Protein Analysis
(by DAN cluster)
PPM2/3
PAL
ΔF
p=0.08
TH,R58-GAL4 X UAS-RNAi
L
Cell Number
(by DAN cluster)
PPM2/3
PAL
ns
TH+ neurons/hemisphere
TH,R58-GAL4 X UAS-RNAi

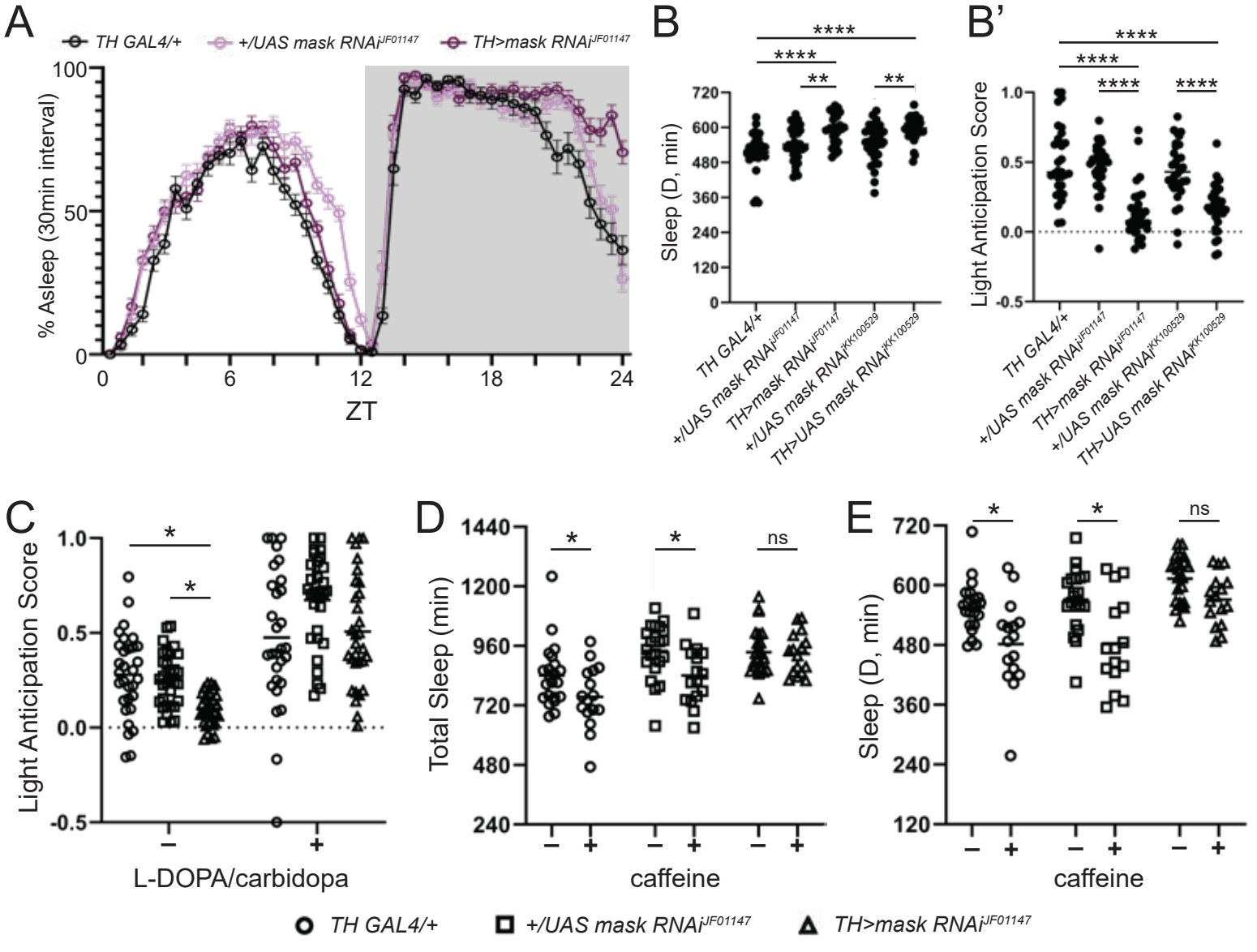
A
TH GAL4/+
+/UAS mask RNAi^JF01147
TH>mask RNAi^JF01147
% Asleep (30min interval)
ZT
B
Sleep (D, min)
TH GAL4/+
+/UAS mask RNAi^JF01147
TH>mask RNAi^JF01147
+/UAS mask RNAi^KK100529
TH>UAS mask RNAi^KK100529
B'
Light Anticipation Score
C
Light Anticipation Score
L-DOPA/carbidopa
D
Total Sleep (min)
caffeine
E
Sleep (D, min)
caffeine
TH GAL4/+
+/UAS mask RNAi^JF01147
TH>mask RNAi^JF01147